THE ASTROPHYSICAL JOURNAL SUPPLEMENT SERIES, 85:411–432, 1993 April

BIDIRECTIONAL ~1 MeV amu^{-1} ION INTERVALS IN 1973–1991 OBSERVED BY THE GODDARD SPACE FLIGHT CENTER INSTRUMENTS ON *IMP 8* AND *ISEE 3/ICE*

I. G. RICHARDSON[1] AND D. V. REAMES
Laboratory for High Energy Astrophysics, NASA/Goddard Space Flight Center, Greenbelt, MD 20771
Received 1992 May 7; accepted 1992 August 31

ABSTRACT

A search has been made for bidirectional energetic ion flows (BIFs) in the solar wind at 1 AU during 1973–1991 using ~1 MeV amu^{-1} ion data from the Goddard Space Flight Center instruments on *ISEE 3/ICE* and *IMP 8*. Some 4000 intervals have been identified. These range in duration from ~15 minutes to over 60 hr (mean = 3 hr), corresponding to scale sizes from ~0.003 to >0.7 AU. The occurrence rate falls off exponentially with an *e*-folding duration of ~4 hr (~0.05 AU). BIFs are observed more frequently around solar maximum, when they are observed ~12% of the time compared with ~5% at solar minimum. Intervals with durations greater than 4 hr are observed on average approximately every 3–4 days at solar maximum and every 2 weeks at solar minimum, with ~33% of these intervals following within 2 days of an interplanetary shock. Around 80% of previously reported bidirectional >35 keV ion flows, bidirectional solar wind electron heat fluxes, magnetic clouds and He enhancements, signatures attributed to the passage of coronal mass ejections (CMEs), show evidence of bidirectional >1 MeV amu^{-1} BIFs. Of the other 20%, around half are associated with low energetic ion fluxes, and the remainder with solar particle events and shock-accelerated ions which do not show bidirectional streaming. These various CME signatures and the >1 MeV amu^{-1} BIFs usually do not coincide exactly, however, and additional bidirectional ion events are identified. A one-to-one association between individual BIFs and CMEs does not occur. In particular, intermittent episodes of ion bidirectionality may occur during the passage of clear magnetic cloud signatures. Hence CME boundaries and durations may not be identified unambiguously from BIF observations.

Subject headings: interplanetary medium — solar wind — Sun: particle emission

1. INTRODUCTION

We report on the results of a survey of bidirectional field-aligned energetic ion flows (BIFs) observed in the solar wind at ~1 AU covering the interval 1973 October to 1991 February. This study uses 15 minute and 2 hr averaged ~1 MeV amu^{-1} ion anisotropy data from the GSFC instruments on the *ISEE 3/ICE* and *IMP 8* spacecraft which have recently become available for analysis. The study complements the previous survey by Marsden et al. (1987) of 35–1000 keV ion data from the *ISEE 3/ICE* spacecraft which identified 66 BIFs with durations > 3 hr between 1978 August and 1982 April. In particular, it extends the time period over which BIF surveys have been performed to around 1.5 solar cycles, thereby allowing the solar cycle variation to be investigated. Preliminary results were reported by Richardson & Reames (1991). However, the analysis here has been refined, in particular for the *IMP 8* data where additional intervals have been identified and BIFs during noninterplanetary periods removed.

BIFs in the interplanetary medium may originate in various ways, most simply from the superposition of independent ion populations flowing in opposite directions along the magnetic field. For example, a spacecraft on a field line connected to Earth's bow shock may detect Sunward-streaming particles reflected or accelerated at the bow shock simultaneously with particles streaming away from the Sun. Or, a solar particle event may commence at a time when particles streaming Sunward from an interplanetary shock in the outer heliosphere are already present. Also, local fluctuations in the solar wind magnetic field may reflect particles, producing a bidirectional flow. In addition, particle trapping may also set up a bidirectional flow. For example, Balogh & Erdös (1983) discussed a bidirectional 35–1600 keV ion flow on field lines which intersected an approaching shock at two places, the ions being trapped and reflected by the shock. Particle trapping may also occur within large-scale solar wind structures such as the magnetic field loops rooted at the Sun ("magnetic bottles") proposed by Morrison (1954), Cocconi et al. (1958), Gold (1959), or closed magnetic field structures ("plasmoids") formed by the disconnection of the magnetic field loops from the Sun (Piddington 1958). Several bidirectional ion flow events closely following interplanetary shocks have been discussed by Rao et al. (1967), Palmer, Allum, & Singer (1978), Kutchko et al. (1982), Sarris & Krimigis (1982), Sanderson et al. (1983), Tranquille et al. (1987), and Sanderson et al. (1990). Most of these authors interpreted the bidirectional flows as indicative of plasmoid or magnetic bottle-like structures within shock drivers. A different interpretation, however, that postshock bidirectional ion flows arise on "open" field lines from particle reflection between the field convergence behind the shock front and the Sun, was favored by Rao et al. (1967) and discussed recently by Kahler & Reames (1991). Bidirectional ion flows are of interest therefore because they may provide information on large-scale structures in the solar wind.

Many interplanetary shock drivers are clearly associated

[1] Also Department of Astronomy, University of Maryland, College Park, MD 20742

with coronal mass ejections (CMEs) (Wilson & Hildner 1986), which have been studied close to the Sun for many years using coronagraphs (see the reviews by Hundhausen 1988 and Kahler 1987, 1988). However, other CMEs apparently do not drive shocks. If CMEs drag out solar magnetic flux, forming expanding loops of magnetic field rooted at the Sun (which may subsequently disconnect from the Sun forming plasmoid-like structures), then BIFs may be expected to be a characteristic interplanetary signature associated with CMEs. (On the other hand, the detection of a BIF does not necessarily indicate the presence of a CME for the reasons given above.) Other signatures attributed to the passage of CMEs (Zwickl et al. 1983; Gosling 1990 and references therein) include solar wind enhanced helium abundances, depressed ion and electron temperatures, unusual ionization states, strong magnetic fields with low variances and smooth rotations characteristic of magnetic clouds, and bidirectional solar wind electron heat fluxes, as well as cosmic-ray Forbush decreases (Sanderson et al. 1990). We find a good (but not complete) association between these signatures and bidirectional ion flows, suggesting that BIFs are found in association with a majority of CMEs. However, the intervals where these various signatures and BIFs are observed clearly do not coincide exactly, and we demonstrate that there is not a simple one-to-one correspondence between BIFs and CMEs.

In § 2, we describe the instrumentation and data analysis, and indicate some of the advantages and limitations of the data as a means of identifying BIFs in the solar wind. Section 3 discusses the BIF observations which are summarized in § 4.

2. INSTRUMENTATION AND DATA ANALYSIS

The GSFC experiment on *IMP 8* (McGuire von Rosenvinge, & McDonald 1986) includes the Low Energy Detector (LED) which detects >0.5 MeV amu^{-1} ions within a viewing cone ± 25° from the ecliptic with a geometrical factor of 0.39 cm^2 sr, and the Very Low Energy Telescope (VLET) which detects >1.7 MeV amu^{-1} ions within 18° of the ecliptic and has a geometrical factor of 0.16 cm^2 sr. *IMP 8* was launched in 1973 October into a 12.5 day period geocentric orbit with an apogee of 40 R_E and a perigee of 30 R_E. The spacecraft was in the solar wind upstream of Earth's bow shock for ~60% of each orbit.

The GSFC medium energy cosmic ray experiment on *ISEE 3/ICE* (von Rosenvinge et al. 1978) consists of two high-energy telescopes (HETs) which detect >4 MeV amu^{-1} ions and 0.2–2 MeV electrons, and two Very Low Energy Telescopes (VLETs) which detect 1–4 MeV amu^{-1} ions. The HETs and VLETS have fields of view of ±25° from the ecliptic and geometrical factors of 0.8 cm^2 sr and 0.28 cm^2 sr, respectively. Following launch in 1978 August, *ISEE 3/ICE* orbited the Sun-Earth L1 libration point 1.5 million km upstream of Earth from 1978 November until 1982 September. From late 1982 December to 1983 December, the spacecraft was largely in the geomagnetic tail. In 1983 December it was placed in a ~1 AU heliocentric orbit in which it advanced ahead of Earth by ~10° heliolongitude per year. The *ISEE 3/ICE* data coverage deteriorated significantly after this time, from >90% to ~14% in 1987.

BIFs have been identified using the following data: for *ISEE 3/ICE*, VLET 1–4 MeV amu^{-1} $Z \geq 1$ and $Z = 2$ ion data and HET > 4 MeV amu^{-1} $Z \geq 1$ and $Z = 2$ ion data from launch to 1990 (15 minute averaged data) or 1991 February (2 hr averaged data). For *IMP 8*, 2 hr averaged 0.5–4 MeV amu^{-1} $Z = 1$, 2 ion, 4–22 MeV amu^{-1} $Z = 1$, 2 ion and 1.7–12 MeV amu^{-1} $Z \geq 2$ ion data from intervals when the spacecraft was in the solar wind from launch to 1989 December. For each energy channel, particle counts are accumulated in eight sectors in azimuth as the spacecraft spins and fitted to a third-order Fourier series in azimuth (Φ)

$$I(\Phi) = A_0\{1 + \sum_{n=1,3} A_n \cos n(\Phi - \Phi_n)\}$$

(Zwickl & Webber 1976). BIFs are characterized by a large second harmonic (A_2) compared to the first and third harmonics (A_1 and A_3). In particular, we require $A_2/A_1 > 0.8$, $A_2/A_3 > 2.0$, and $A_2 > 0.1$ (to remove nearly isotropic intervals) together with more than 20 accumulated counts. The bidirectional flow direction (Φ_2) is also required to be aligned less than 45° from the average magnetic field azimuth in the same averaging interval (which is required to have a standard deviation of less than 45° to remove intervals with large changes in field direction). These criteria were developed to select intervals which were judged to be BIFs from examining pie plots of the sectored intensities (such as will be presented below).

Several points should be noted about the data: since the particle observations are made in a limited viewing range centered on the ecliptic, the complete pitch-angle distribution is not sampled when the magnetic field has a large out-of-the-ecliptic component. In practice, BIFs can generally be identified at such times (although the harmonic amplitudes obtained will not accurately represent those of the complete distribution). The data have not been transformed into the solar wind frame since at the energies considered here, the change in the particle distribution on transformation (in particular, in the second harmonic) is not sufficient to affect significantly the intervals identified. Also, to attempt to allow for data gaps and intermittent bidirectionality within events (as discussed below), bidirectional intervals separated by less than 3 hr are assumed to form part of the same event.

Although the data span over 1.5 solar cycles, allowing the solar cycle variation of BIFs to be examined, several systematic effects may influence the apparent BIF rate over this interval. In the case of *IMP 8*, the LED anticoincidence shield failed in 1984 April, resulting in the 4–22 MeV amu^{-1} channel becoming unreliable (R. E. McGuire 1991, private communication). However, this has no obvious effect on the BIF detection efficiency. For *ISEE 3/ICE*, the reduced data coverage after 1983 influences both the BIF detection rate and duration. Typically, the spacecraft was tracked only for several (~4–6) hr each day. Since BIFs generally have durations of several hours, the restricted data coverage may set an upper limit to the observed duration. Also, no VLET data are available from 1988 July to 1989 January (the HET data are less sensitive to BIFs), and no HET data after 1989 January. In addition, only limited magnetic field data are presently available after 1987 January, so some of the BIFs identified may in fact be "pancake" distributions, peaked at large pitch angles, associated, for example, with shock-drift acceleration at interplanetary shocks (Decker 1983) and particle mirroring. We have not included in the analysis BIFs in the vicinity of ion enhancement peaks which may be associated with shocks, and estimate (based on observations when field data are available) that only ~20% of the BIFs identified after 1987 are likely to be due to pancake distributions.

In the L1 orbit, *ISEE 3/ICE* was generally free of magnetospheric effects. Occasionally, >35 keV ions streaming upstream from Earth's bow shock were observed (Sanderson, Reinhard, & Wenzel 1981) but these were not significant at the energies considered here. Also, a comparison of the *ISEE 3/ICE* > 1 MeV amu^{-1} BIFs identified in 1978–1981 with >35 keV ion data from the EPAS instrument on *ISEE 3/ICE* suggests that there is no general association with the presence of upstream ions, which indicates that the bidirectional flows do not arise from simultaneous observation of magnetospheric and antisolar streaming ions. At *IMP 8,* upstream ions are more likely to be present than at *ISEE 3/ICE* since the spacecraft is connected more frequently to the bow shock. However, again, at the energies considered here, upstream ions do not pose a significant problem. Energetic ions must also be present in sufficient numbers to enable their distribution to be examined and bidirectional flows to be identified. For 2 hr averaged data, the >20 counts per integration period criterion is exceeded for 86% (83%) of the *ISEE 3/ICE* (*IMP 8*) intervals. Bidirectional flows may also be obscured if a dominant streaming or near-isotropic ion population is present, for example, accelerated by an energetic solar event or an interplanetary shock. In summary, although the presence (or absence) of a bidirectional ion flow can provide an important indicator of the presence of solar wind structures such as CMEs, it must be recognized that the data are subject to other influences which may affect the observability of bidirectional flows.

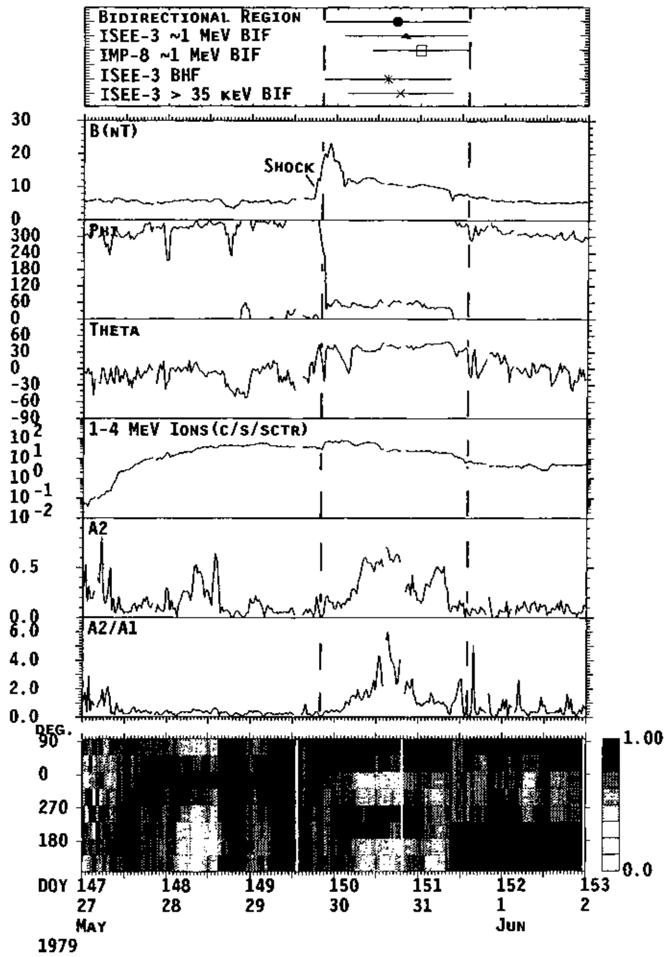

FIG. 1.—Example of a bidirectional ion flow (BIF) at *ISEE 3/ICE* on 1979 May 29–31.

3. OBSERVATIONS

3.1. *Example of a* ~1 MeV amu^{-1} *BIF*

Figure 1 shows *ISEE 3/ICE* observations of a particularly clear bidirectional ion flow on 1979 May 29–31 (also discussed by Marsden et al. 1987) following passage of a shock at 1818 UT on 1979 May 29. The top panel indicates *ISEE 3/ICE* and *IMP 8* ~1 MeV BIF intervals identified in our survey together with the intervals over which a solar wind electron bidirectional heat flux (BHF) (Gosling et al. 1987) and a >35 keV ion BIF (Marsden et al. 1987) were observed. The next three panels show the magnetic field intensity, and azimuthal and polar angles. The fourth panel shows the flux of 1–4 MeV amu^{-1} ions (in units of counts s^{-1} per azimuthal sector). The fifth and sixth panels display the magnitude of the second harmonic A_2 and the ratio of the second and first harmonics, A_2/A_1 for the 1–4 MeV amu^{-1} ions. The gray scale shows 1 hr averaged ion intensities in the eight azimuthal sectors, normalized to the sector with the highest intensity and plotted versus viewing direction such that a dark band around 0° corresponds to radial antisolar flow.

An interval of ion bidirectionality, indicated by a large value (>0.8) of A_2/A_1 and double bands of dark shading separated by ~180°, is apparent at *ISEE 3/ICE* for the nearly 35 hr interval from ~0215 UT on May 30 to ~1300 UT on May 31. Integrating the solar wind speed during this interval indicates a scale size of ~0.37 AU. The *ISEE 3/ICE* and *IMP 8* ~1 MeV BIF intervals coincide reasonably well with the >35 keV and BHF intervals. However, the start and finish times do differ by several hours, so there is clearly not exact agreement. (In the case of *IMP 8,* the later onset is due to the spacecraft being in the magnetosphere at the start of the interval). Taking the observations together, the region of bidirectional flows corresponds to a plasma structure with an enhanced magnetic field directed nearly perpendicular ($\Phi \sim 60°$) to the average spiral magnetic field azimuth ($\Phi = 135°$) and inclined ~45° north of the ecliptic. This presumably forms the driver of the May 29 shock, but would not be classified as a magnetic cloud due to the absence of a distinct magnetic field rotation within the structure.

3.2 *Durations and Occurrence Rates of* >1 MeV amu^{-1} *BIFs*

Some 1995 BIFs have been found in the *ISEE 3/ICE* data from 1978 August to 1991 February, and 2156 events in the *IMP 8* data between 1973 October and 1989 December. Figure 2 shows frequency distributions for the BIF durations at *ISEE 3/ICE* (grouped in 15 minute and 2 hr bins) and *IMP 8* (2 hr bins). These indicate that brief BIFs were observed (as Marsden et al. (1987) also noted in passing) in addition to those extending many hours (such as that shown in Fig. 1) empha-

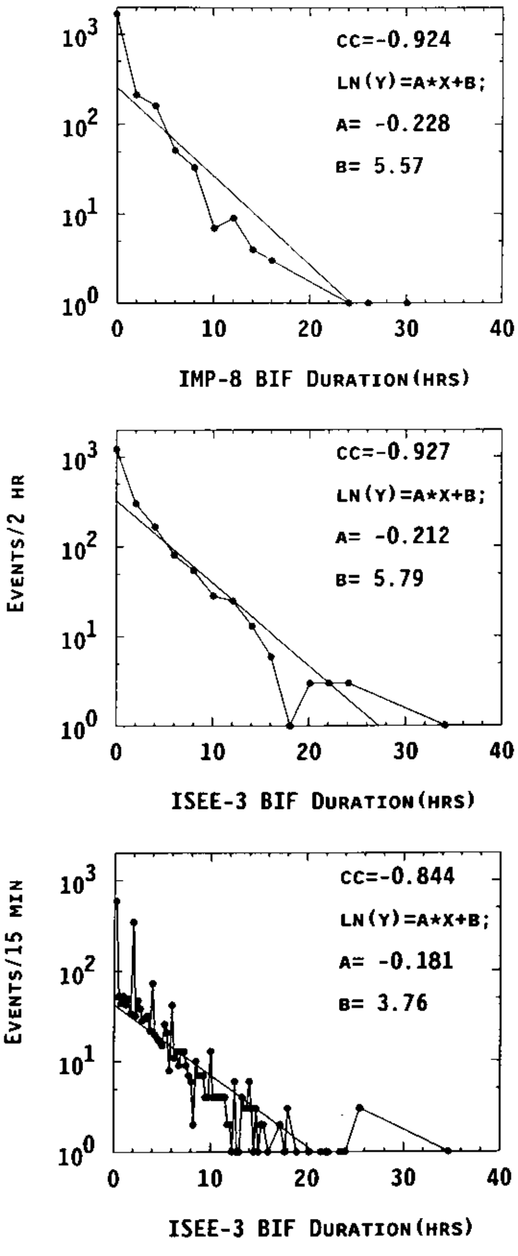

FIG. 2.—Frequency distributions of BIF durations at *IMP 8* (top panel) and *ISEE 3/ICE* (grouped into 2 hr and 15 minute bins [*middle and bottom panels*]). The log-linear fits and correlation coefficients are indicated.

sized by previous studies. The durations extend from the minimum 15 minute (*ISEE 3/ICE*) or 2 hr (*IMP 8*) data averaging interval (corresponding to scale sizes of ~0.003–0.02 AU) to over 20 hr (>0.2 AU). The occurrence rates decline approximately exponentially with duration, with *e*-folding durations of ~3.8 hr at *IMP 8* and 4.7 hr at *ISEE 3/ICE* (corresponding to scale sizes of ~0.05 AU). It should be noted that the distributions are dependent somewhat on the interval chosen to group intervals into the same event (here 3 hr) and so may not precisely reflect the true distribution of BIF scale sizes in the solar wind. The mean durations are 2.9 ± 2.3 hr at *IMP 8* and 2.8 ± 3.4 hr at *ISEE 3/ICE* (the large errors reflecting the variation in duration, with many short duration events and a few longer events).

The BIFs identified at *ISEE 3/ICE* together have a total duration of 5546 hr (231 days), equivalent to ~10% of the observing time (after allowing for spacecraft data coverage) and ~12% of the time with an ion flux > 20 counts per 2 hr. The 30% of intervals having durations greater than 3 hr contribute 72% of this total however, so overall, the longer events extending many hours are more important generators of bidirectional flows. At *IMP 8*, 6317 hr (263 days) of bidirectional flows have been identified, amounting to ~9% of the observing time in the solar wind.

Figure 3 shows the durations of the bidirectional ion events identified at *IMP 8* and *ISEE 3/ICE* during 1974–1989, together with the yearly averaged spacecraft data coverage in the solar wind. There is some evidence of a solar cycle effect, with BIFs tending to occur more frequently, and to be of longer duration, around solar maximum in 1981 and approaching the 1990 solar maximum. At *ISEE 3/ICE*, however, the fall in data coverage after 1983 followed by the slight rise in 1988–1989 (when the spacecraft was off the west limb of the Sun and obtained increased tracking) also contribute to this variation, while the limited data coverage in the late 1980s suppresses BIFs extending more than a few hours, as discussed in § 2.

Figure 4 shows the daily-averaged occurrence rates for BIFs of various durations corrected for changing spacecraft coverage. In general, the occurrence rates of BIFs with durations from less than 2 hr to ~1 day show some correlation with solar

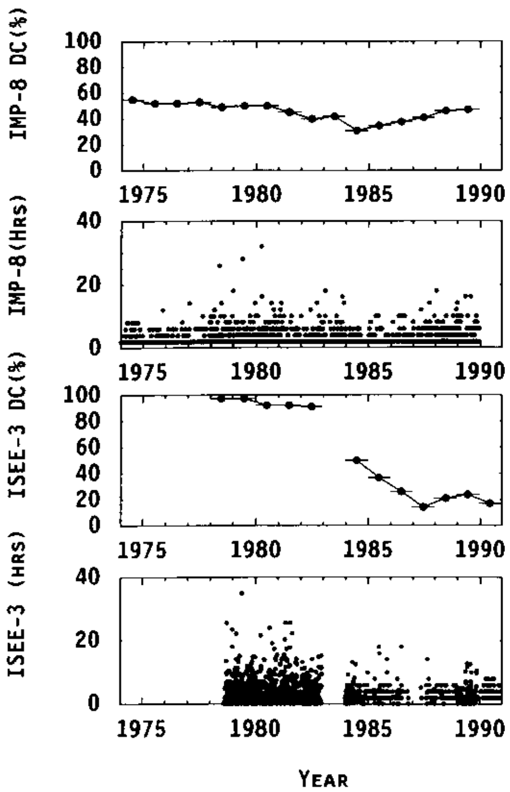

FIG. 3.—Spacecraft data coverage (in the solar wind) and BIF durations for *IMP 8* (*top two panels*) and *ISEE 3/ICE* (*bottom two panels*).

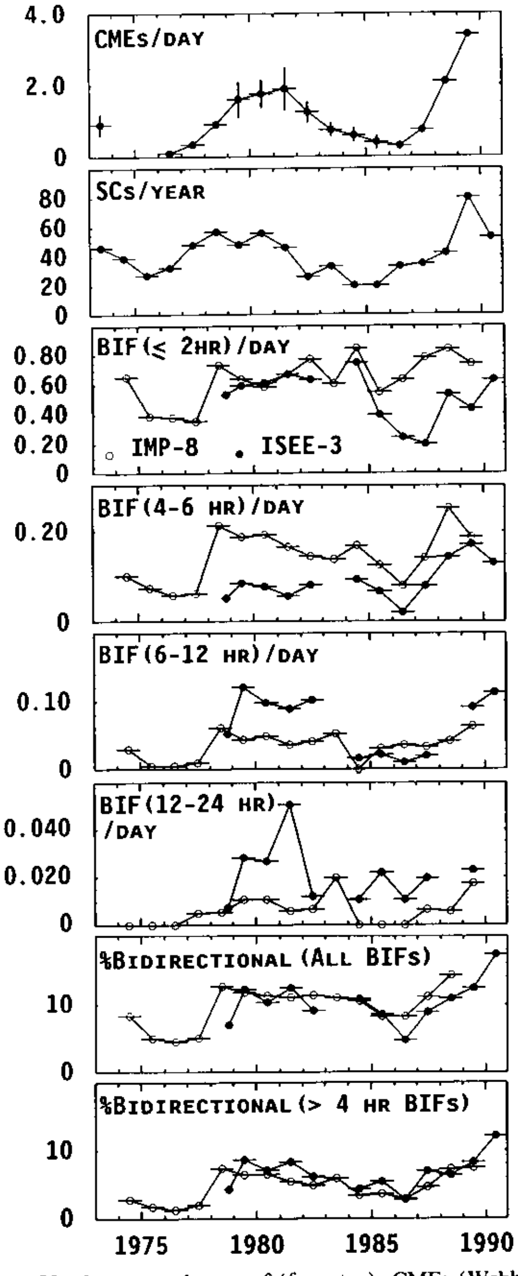

FIG. 4.—Yearly averaged rates of (*from top*): CMEs (Webb 1991); SSCs (Solar-Geophysical Data); ≤2 hr, 4–6 hr, 6–12 hr, and 12–24 hr duration BIFs at *IMP 8* (open circles) and *ISEE 3/ICE* (filled circles) (corrected for spacecraft coverage). The bottom two panels show the percentage of the observation time in the solar wind when BIFs associated with all events and >4 hr duration events were present.

activity, tending to be highest during solar maximum conditions around 1980 and 1990. They are also reasonably comparable at both spacecraft even though the instruments and data-averaging intervals are not completely identical. Figure 4 also shows the percentage of the observing time when bidirectional events were evident at each spacecraft, both for all BIFs and for those with durations greater than 4 hr. Again, there is a solar cycle variation, with BIFs being observed ~12% of the time during and following solar maximum in 1978–1984 (and possibly more frequently during the late 1980s approach to solar maximum), compared to ~5% at solar minimum. BIFs with durations of less than 4 hr are observed ~8% of the time at solar maximum and ~2%–5% at solar minimum.

Solar cycle variations are also evident in the CME rate observed by coronagraphs (Webb 1991) and in the number of geomagnetic storm sudden commencements (SSCs) each year (from Solar-Geophysical Data) (taken as an indication of the rate of interplanetary shock production), plotted in the top two panels of Figure 4. The variations in BIF rate apparently reflect variations in the CME and SSC rates, as might be expected if BIFs show some association with CMEs/shock drivers. To show this more explicitly, BIF occurrence rates (corrected for spacecraft coverage) plotted versus the CME rate are shown in Figure 5 together with weighted least-squares fits to the data. The top two panels for each spacecraft show the rates of <2 hr and >4 hr duration BIFs while the bottom panels show the percentage of the observing time that BIFs were observed, the right-hand panel including only greater 4 hr duration events. At both spacecraft, the >4 hr BIF rate and the percentage of the time that BIFs are observed are correlated with the CME rate, consistent with (but not proving) an association between BIFs and CMEs. The <2 hr duration BIFs show a weaker correlation. This may indicate that the briefer BIFs may also arise from effects which do not show a solar cycle dependence, such as reflection by fluctuations in the solar wind magnetic field.

Figure 6 shows the *IMP 8* and *ISEE 3/ICE* BIF rates plotted versus the rate of SSCs (which are generally associated with the passage of interplanetary shocks). The positive correlations are less clear than in Figure 5, but still evident (except for <2 hr duration BIFs where no trend is apparent). The occurrence rate of >4 hr duration BIFs is around twice the SSC rate, indicating that no more than 50% of >4 hr duration BIFs are associated with SSCs.

Gosling et al. (1992) demonstrated that the occurrence of *ISEE 3/ICE* bidirectional solar wind electron heat fluxes also shows a clear dependence on solar activity, and it is interesting to compare their results with the BIF observations. Figure 7 shows the yearly averaged percentage of solar wind measurements with bidirectional heat fluxes (from Gosling et al. 1992) together with the percentage of the time that BIFs were observed at *IMP 8* and *ISEE 3/ICE* (from Fig. 4). These show both similarities and differences. Bidirectional ion and solar wind heat fluxes were observed for similar fractions of the time prior to the 1980 solar maximum (~6%) and during solar maximum conditions (~12%–15%). However, bidirectional ion flows were observed more frequently than bidirectional electron heat fluxes during the mid-1980s solar minimum (although a minimum rate was reached in 1986 in all cases), and the fall-off in the bidirectional heat flux rate in 1990 is not evident in the *ISEE 3/ICE* ion data. Overall, though, these three independent data sets appear to concur in showing evidence of a solar cycle variation of bidirectional flow occurrence in the solar wind at 1 AU ranging from ~15% at solar maximum to ~1%–5% at solar minimum.

Gosling et al. (1992) have also estimated the year-by-year number of CMEs expected at a point in the ecliptic plane using the SMM coronagraph observations of St. Cyr & Burkepile (1990). They estimate a rate of ~60–70 events per year (0.16–

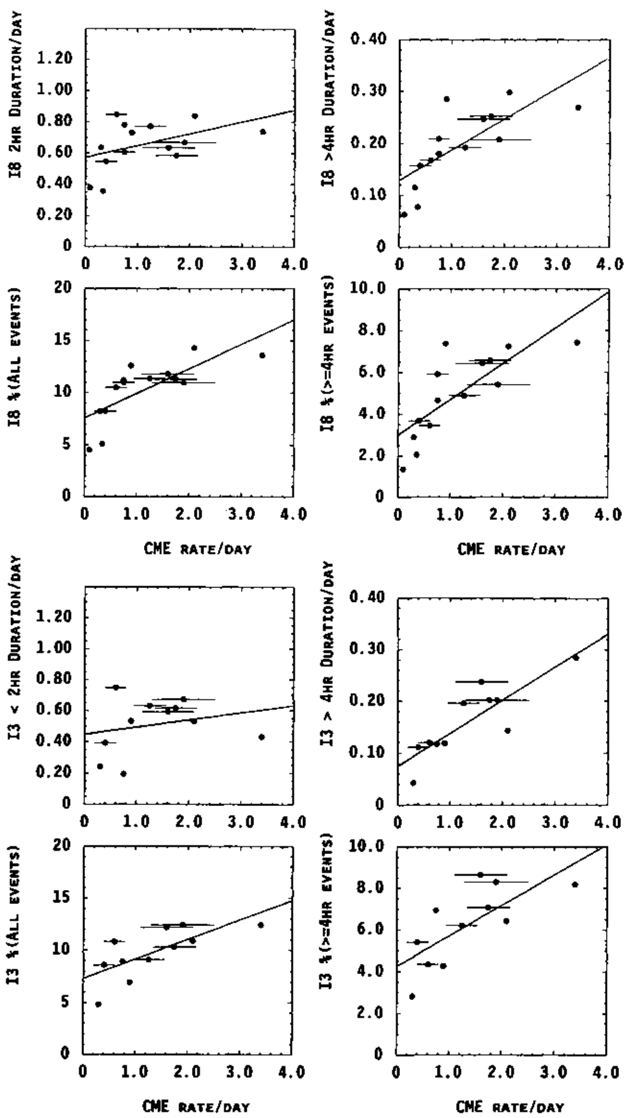

FIG. 5.—BIF occurrence rates at both spacecraft (from Fig. 4) vs. CME rate at the Sun (Webb 1991).

0.19 events per day) at solar maximum, falling to ~10 events per year (~0.03 events per day) at solar minimum, and note that these rates are consistent with their observed rate of bidirectional heat flux events, assuming a one-to-one association between BHFs and CMEs. The estimated CME rate is consistent with, but around a factor of 2 or so lower than the ≥4 hr duration BIF event rates in Figure 5, suggesting that although BIFs and CMEs may indeed be related, there is not a clear one-to-one association.

3.3 *BIF Observations, 1978 August 15–October 7*

Figure 8 places in context *IMP 8* and *ISEE 3/ICE* BIFs with durations ≥ 1 hr identified during the first two solar rotations following *ISEE 3/ICE* launch (Bartels rotations 1983–1984, 1978 August 15–October 7) which are representative of our observations. The *ISEE 3/ICE 1–4* MeV amu^{-1} ion intensity (in the top panel for each solar rotation) is dominated by enhancements associated with the passage of interplanetary shocks produced by energetic solar events. Near-Earth solar wind plasma parameters (from the NSSDC OMNI data base; (Couzens & King 1986) are also shown, together with solar wind electron BHFs from Gosling et al. (1987), >35 keV BIFs (Marsden et al. 1987) and magnetic cloud observations from Zhang & Burlaga (1988). The *ISEE 3/ICE* and *IMP 8* BIFs show a fair, but certainly not exact agreement with the BHF, >35 keV BIF, and magnetic cloud intervals and with each other. Consistent with Figure 6, around one half are observed within 2 days following passage of an interplanetary shock (or of a shocklike structure in the solar wind associated with an SSC) and may indicate the shock driver. It is evident from the shock drivers on August 27–28, September 10 and 29–30, and October 4–5 that the intervals of ion and electron bidirectionality and magnetic cloud signatures, where present, do not usually coincide precisely and that bidirectional ions may in fact only be observed intermittently within these intervals. Also, on occasion, a region including bidirectional electron heat fluxes is not identified in the ion data due to low ion fluxes (e.g., September 20). On the other hand, ~1 MeV BIFs are also found where bidirectional >35 keV ions and electron heat

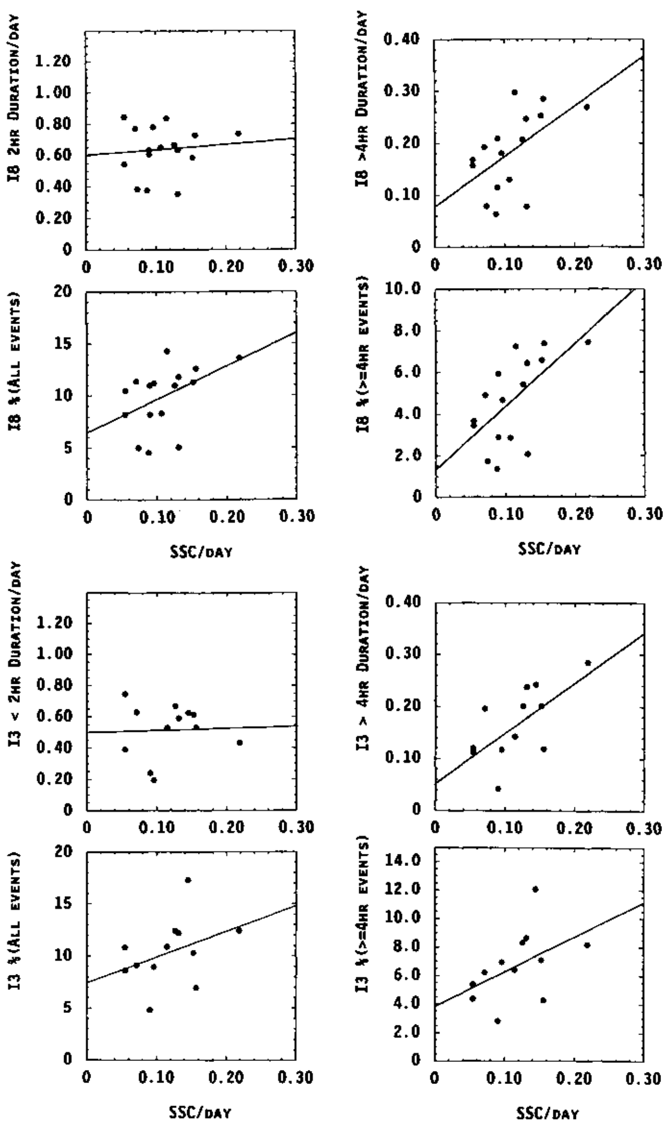

FIG. 6.—BIF occurrence rates at both spacecraft vs. SSC rate

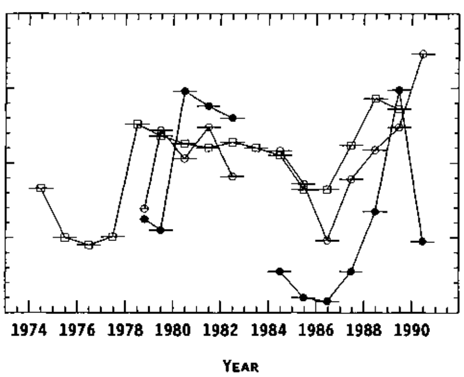

FIG. 7.—Percentages of the time when bidirectional ~1 MeV ions were observed at *IMP 8* (*open squares*) and *ISEE 3/ICE* (*open circles*), and bidirectional solar wind electron heat fluxes (Gosling et al. 1992) were observed at *ISEE 3/ICE* (*filled circles*).

fluxes have not been reported. Several of these BIFs are associated with small-scale plasma features with no preceding shocks, characterized by localized plasma temperature depressions, or occur within longer term temperature depressions, as indicated in the figure. The temperature depressions suggest that these BIFs may be associated with expanding CME-like plasma structures and do not occur at random. Finally, the energetic ion flux often shows depressions following shock passage in the vicinity of (but not always exactly coincident with) the bidirectional regions associated with shock drivers, as noted for example by Marsden et al. (1987).

3.4. *Association of CME Signatures with* ~1 MeV amu^{-1} *Ion BIFs*

We now consider the association of previously reported signatures of CMEs with ~1 MeV amu^{-1} ion BIFs. Table 1 shows the percentage of events identified in various surveys of CME-like signatures in the near-Earth interplanetary medium which show evidence of bidirectional ~1 MeV amu^{-1} ion flows during at least part of the interval over which the signature has been reported. The number of events, given in column (2), takes into account data gaps in the ion observations and hence may differ slightly from the number of events cited in the surveys. In most cases, there is a close association, with typically more than 80% of the events in these surveys being associated with BIFs. As might be expected, there is a particularly close association with the >35 keV ion BIF survey of Marsden et al. (1987). An exact correspondence with these various surveys does not occur, however, principally for two reasons.

First, there are occasions when the energetic ion population clearly *does not* show a bidirectional flow at the time when a CME signature is reported. This generally occurs when ions accelerated by an energetic solar event or by an interplanetary shock (in particular in the vicinity of the spacecraft) dominate the energetic ion population. Typically either a unidirectional streaming (away from the Sun or the shock) or a near-isotropic distribution is observed. Figures 9 (in a format similar to Fig. 1 but without the gray-scale intensity plot) and 10 show an example of a clearly nonbidirectional ion distribution observed at the time of a BHF identified by Gosling et al. (1990). The reported interval of bidirectional solar wind heat flux (1982 February 2, 1100–2330 UT) is delineated by the vertical dashed lines in Figure 9. This occurred during a long duration energetic ion event which commenced on 1982 January 29 and extended beyond February 6. The BHF follows a shock (evident in the magnetic field intensity data) which passed by *ISEE 3* at 1035 UT on February 1 (Gosling et al. 1990) and

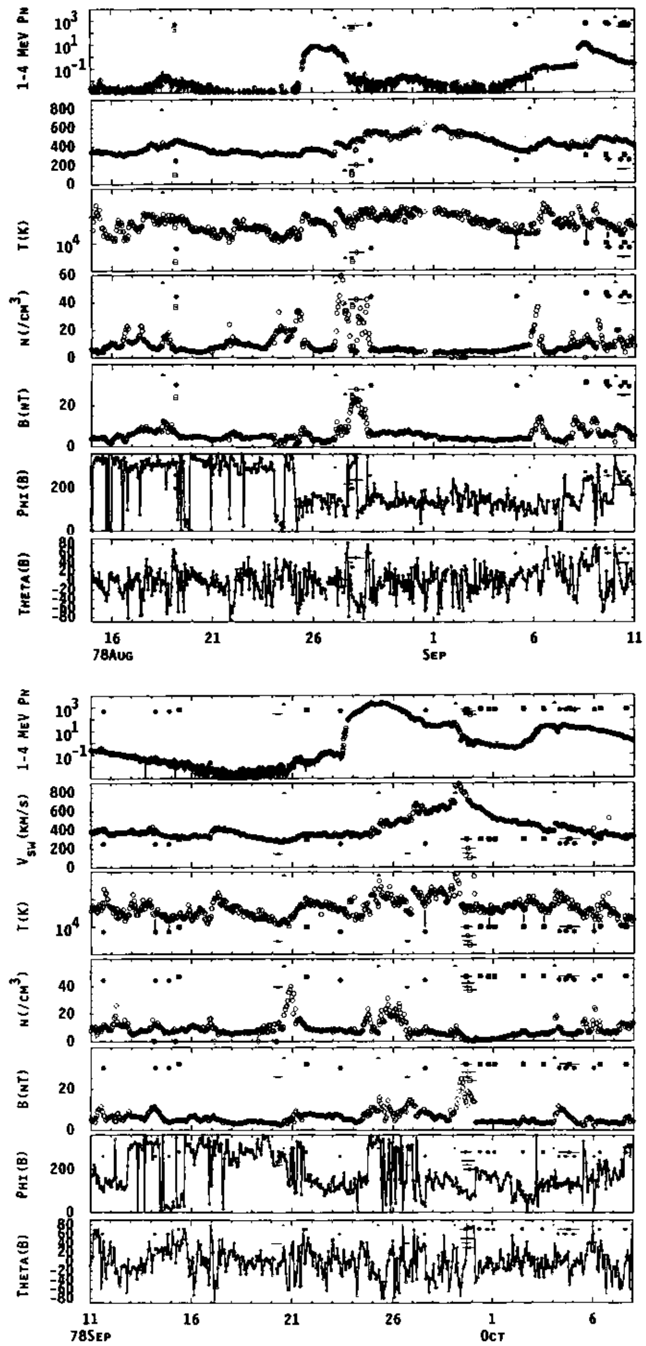

FIG. 8.—BIFs at *IMP 8* (*solid circles*) and *ISEE 3/ICE* (*solid squares*) observed during the first two solar rotations after the launch of *ISEE 3/ICE* (1978 August 15–October 7), plotted in relation to near-Earth solar wind parameters (speed, proton temperature, density, and magnetic field strength) and the 1–4 MeV amu^{-1} ion intensity. Solar wind electron bidirectional heat flux events (*open triangles*), >35 keV ion BIFs (*open squares*), magnetic clouds (*open circles*), and interplanetary shocks/SSCs (*solid triangles*) are also indicated.

TABLE 1

ASSOCIATION OF CME SIGNATURES AND >1 MeV BIFs

Signature	Events	Events with >1 MeV BIFs	Percent BIF Associated
He Enhancement			
Borrini et al. 1982a	31	18 (+8N, 5L)*	58% (+26%N, 16%L)*
Neugebauer & Alexander 1991	17	16 (+1L)	94% (+6%L)
Magnetic Cloud			
Zhang & Burlaga 1988	19	16 (+3L)	84% (+16%L)
Lepping et al. 1990	14	11 (+1N, 2L)	79% (+7%N, 14%L)
Bidirectional Solar Wind Electron Heat Flux			
Gosling et al. 1987	49	32 (+6N, 11L)	65% (+13%N, 22%L)
Gosling et al. 1990	31	27 (+2N, 2L)	88% (+6%N, 6%L)
Gosling 1989	147	111 (+25N, 11L)	76% (+17%N, 7%L)
>35 keV Ion BIF			
Marsden et al. 1987	66	61 (+1N, 4L)	92% (+2%N, 6%L)
(Class 1a-Shock + B rotation)	19	17 (+2L)	89% (+11%L)
(Class 1b-B rotation only)	8	7 (+1L)	87% (+13%L)
(Class 2a-Shock, no B rotation)	12	11 (+1L)	92% (+8%L)
(Class 2b-No shock, no B rotation)	9	8 (+1N)	89% (+11%N)
(Class 3-no B structure)	18	18	100%
Forbush Decrease			
Solar Geophysical Data 1990	71	64 (+6N, 2L)	90% (+8%N, 2%L)

NOTES.—N = non-bidirectional ions predominant with streaming or isotropic distributions, L = low ion fluxes, distribution unclear.

was associated with maximum 1–4 MeV ion intensities. The upper panel shows intervals of energetic ion bidirectionality identified in this survey (also using data in addition to the 1–4 MeV ion data shown in the figure) and by Marsden et al. (1987) (>35 keV ions). We note that no bidirectional ions have been identified during the BHF either by Marsden et al. (1987) or from the *ISEE 3*/2ICE data in this study (*IMP 8* was in the magnetosphere). This is also indicated by the small values of A_2 and A_2/A_1 in the lower panels of the figure. However, a brief interval of bidirectionality is apparent at *ISEE 3/ICE* just before the interval given by Gosling et al. (1990). This is shown more clearly in Figure 10 which illustrates pie plots of sectored ion intensities during 30 minute intervals starting at the times indicated on February 2 (DOY 33) prior to and throughout the BHF. The intensities are plotted versus viewing direction with the Sun to the top of the page. The arrows indicate the mean magnetic field azimuth ($\pm 1\ \sigma$) during the data accumulation interval together with the number of counts (several thousand) accumulated in the maximum count sector, to which the data are normalized. The only intervals showing evidence of bidirectionality are those at 0930–1030 UT (corresponding to the BIF in the top panel of Fig. 9 and outlined in Fig. 10 by a thicker box) immediately prior to the BHF. Otherwise, clear field-aligned ion streaming or near-isotropic distributions are associated with the BHF, which commenced at 1100 UT. The absence of bidirectional streaming is not due to the large northward magnetic field excursions evident in Figure 9 taking the bulk of the ion distribution out of the instrumental field of view since streaming/near isotropic distributions are also observed when the field is close to the ecliptic. Bidirectionality is also not reported by Marsden et al. (1987) who used three-dimensional ion data. So in summary, there is clearly an absence of bidirectional ion flows associated with this (and some other) BHFs. Columns (3) and (4) of Table 1 indicate the number of events (N) in each survey where a "nonbidirectional" ion association occurs. The largest numbers of such associations (26%) occur in the He enhancement survey of Borrini et al. (1982) while overall, ~10% of the intervals listed in these CME signature surveys show such an association.

Second, the ion fluxes are too low for the ion flow to be determined reliably, and again Table 1 indicates the number of events in each survey (L) where this occurs. Low fluxes most frequently occur in association with the events in the BHF survey of Gosling et al. (1987) (22%), and on average occur in ~8% of the events in the various surveys. (This is reasonably consistent with ~15% of the data having low fluxes.) Thus overall, we find that ~1 MeV amu^{-1} ion bidirectional flows are observed in ~80% of regions with possible signatures of CMEs but are absent in the other ~20%. We conclude that the occurrence of bidirectional ions, in particular in conjunction with other signatures, provides evidence of the presence of CME structures in the solar wind (although it must also be remembered that bidirectionality can arise for other reasons,

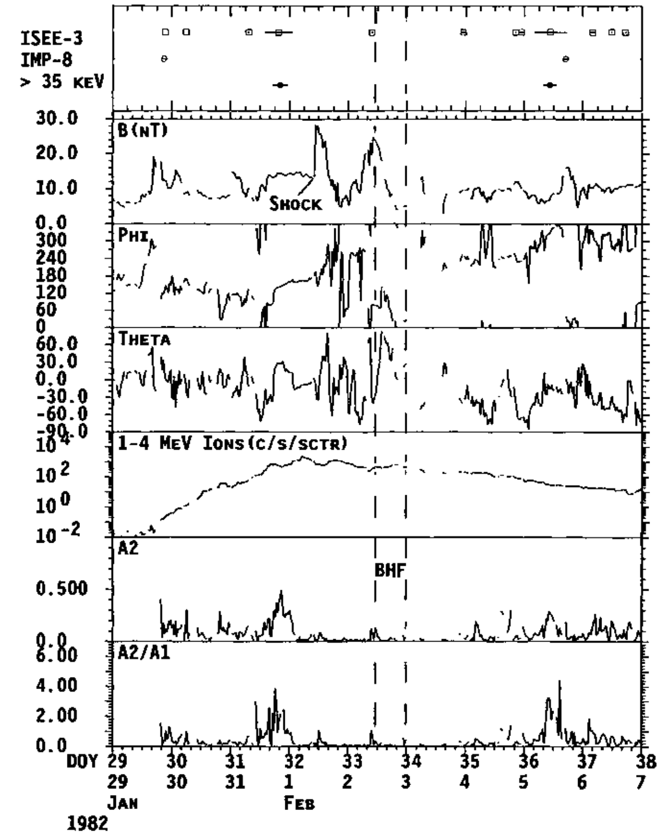

FIG. 9.—*ISEE 3/ICE* observations in the vicinity of a solar wind electron bidirectional heat flux (Gosling et al. 1990) (delineated by dashed vertical lines) on 1982 February 2 which is not associated with bidirectional ions.

as discussed above). However, the absence of bidirectional ions alone does not confirm that a CME was not encountered.

3.5. *>4 Hour Duration Near-Earth BIFS at IMP 8 and ISEE 3/ICE in 1973–1989*

It is not practical here to list all the ~4000 BIFs identified. Instead, in Table 2, we only include BIFs with durations of 4 hr or more observed in the solar wind in the vicinity of Earth from 1973 to 1989 (i.e., only BIFs observed at *ISEE 3/ICE* before 1983, when the spacecraft was largely in the L1 orbit, are considered here in conjunction with the *IMP 8* observations). The *ISEE 3/ICE* observation times have not been adjusted for the ~30 minute solar wind convection time from the L1 orbit to Earth since this is short compared to the BIF duration and comparable to or less than the data averaging period. Where an interplanetary shock (Borrini et al. 1982a; van Nes et al. 1984) and/or SSC (from Solar-Geophysical Data principle magnetic storm and rapid variation reports) was observed less than 2 days prior to a BIF, this is indicated in column (1) of the table. The BIF durations are also given. Column (4) indicates first the spacecraft (*ISEE 3/ICE,* denoted by 3; *IMP 8,* denoted by 8) at which the BIF was observed. Asterisks denote particularly clear events observed simultaneously in three or more ion channels on the same spacecraft. (A few BIFs, observed in three channels but with durations < 4 hr are also included in the table.) We also indicate whether the BIFs were associated with BHFs (Gosling et al. 1987, 1990; Gosling 1989, private communication), denoted by G, bidirectional >35 keV ions (Marsden et al. 1987; Sanderson et al. 1990), denoted by M, solar wind helium enhancements (Borrini et al. 1982b; Neugebauer & Alexander 1991), denoted by He and magnetic clouds (Klein & Burlaga 1982; Zhang & Burlaga 1988; Lepping, Jones, & Burlaga 1990; Farrugia et al. 1992), denoted by C, as well as with Forbush decreases (Solar-Geophysical Data 1990), denoted by F. In many cases, BIFs were observed almost simultaneously at both *ISEE 3/ICE* and *IMP 8,* as would be expected if a region of bidirectional flows with a scale size large compared to the ~0.01 AU spacecraft separation passed by both spacecraft. In all, 834 distinct BIF events (some observed by both spacecraft) are listed, of which ~33% occurred within 2 days of a shock or SSC. Thus, although a significant number of bidirectional intervals are plausibly associated with shock drivers, a majority have no apparent association (as Fig. 6 also indicates). The table also clearly reflects the effects of solar cycle dependence of the BIF occurrence rate and changing spacecraft coverage.

3.6. *Intervals with CME Signatures in 1978 to 1982 Derived from BIF, BHF, and Magnetic Cloud Observations*

As mentioned above, no one signature appears to indicate the exact extent of a bidirectional flow/magnetic cloud region. We have therefore combined our observations with previous BIF, BHF, and magnetic cloud observations for the interval between 1978 August and 1982 December, where the most comprehensive observations are available, in order to identify regions over which these signatures are observed. Table 3 lists times which encompass intervals which are identified independently by more than one bidirectional particle or magnetic cloud signature. In this case, since the intervals are identified using more than one independent data set, we have taken into consideration *ISEE 3/ICE* and *IMP 8* BIFs with >1 hr dura-

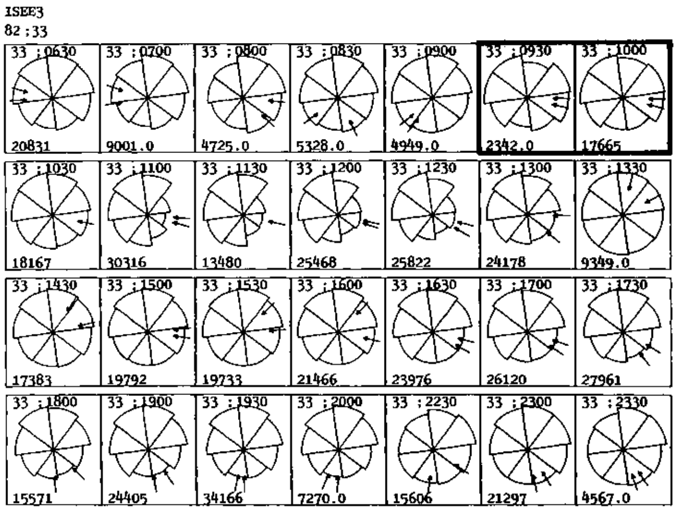

FIG. 10.—Sectored 1–4 MeV amu^{-1} ion intensities prior to and during the bidirectional solar wind heat flux event in Fig. 9 which commences at 11 UT on 1982 February 2 (DOY 33), plotted vs. viewing angle with the magnetic field direction indicated.

TABLE 2

Near-Earth Bidirectional Intervals, ≥4 Hour Duration

Shock	Bi Interval	Duration	S/C
1973			
Nov 5 0954	Nov 5 1700-Nov 6 0100	8.0	8
	Nov 6 0900-Nov 6 1300	4.0	8
1974			
...	Feb 19 1100-Feb 19 1500	4.0	8
...	Mar 19 0500-Mar 19 1100	6.0	8
...	Apr 1 1900-Apr 1 2300	4.0	8
...	Apr 15 1100-Apr 15 1900	8.0	8
...	May 7 1700-May 8 0100	8.0	8F
...	May 16 1100-May 16 1500	4.0	8
...	Jun 1 0500-Jun 1 0900	4.0	8
...	Jun 2 1100-Jun 2 1500	4.0	8
...	Jun 15 1700-Jun 15 2100	4.0	8
Jun 23 0857	Jun 25 0700-Jun 25 1100	4.0	8
Jun 25 2330	Jun 26 0300-Jun 26 0900	6.0	8
...	Jul 3 1700-Jul 4 0100	8.0	8*F
...	Jul 15 2300-Jul 16 0300	4.0	8
...	Aug 15 0900-Aug 15 1300	4.0	8
...	Aug 15 1700-Aug 15 2300	6.0	8
Aug 16 1200	Aug 18 2300-Aug 19 0500	6.0	8
Aug 24 0816	Aug 24 0500-Aug 24 1300	8.0	8
Aug 31 0057	Aug 31 0700-Aug 31 1100	4.0	8
Sep 15 1343	Sep 17 0900-Sep 17 1100	2.0	8*He
Sep 18 1434	Sep 19 0100-Sep 19 0500	4.0	8*
...	Sep 29 2100-Sep 30 0500	8.0	8
...	Oct 3 1700-Oct 3 2100	4.0	8
Oct 12 1244	Oct 13 2300-Oct 14 0700	8.0	8He
...	Oct 31 1700-Oct 31 2100	4.0	8
...	Nov 18 1700-Nov 18 2300	6.0	8
...	Nov 21 0700-Nov 21 1100	4.0	8
Dec 28 0139	Dec 29 2300-Dec 30 0300	4.0	8
1975			
...	Apr 23 0000-Apr 23 0600	6.0	8
...	May 19 0400-May 19 0800	4.0	8
...	Jun 14 1800-Jun 15 0000	6.0	8
Aug 8 0316	Aug 8 1600-Aug 8 2000	4.0	8
	Aug 9 0200-Aug 9 0600	4.0	8
	Aug 9 1400-Aug 9 2000	6.0	8
...	Aug 12 1200-Aug 12 1800	6.0	8
...	Aug 23 1800-Aug 24 0000	6.0	8
Sep 17 0401	Sep 17 1800-Sep 18 0000	6.0	8
...	Sep 19 2200-Sep 20 0200	4.0	8
...	Nov 3 1400-Nov 3 1800	4.0	8
...	Nov 17 0400-Nov 17 0800	4.0	8C
...	Nov 17 2000-Nov 18 0800	12.0	8C
...	Nov 21 0400-Nov 21 0800	4.0	8
Nov 21 2305	Nov 23 0000-Nov 23 0200	2.0	8*
...	Dec 30 1000-Dec 30 1400	4.0	8
1976			
...	Feb 16 1200-Feb 16 1600	4.0	8
...	Feb 23 0200-Feb 23 0800	6.0	8
...	Apr 26 0000-Apr 26 0400	4.0	8
Apr 29 0705	Apr 30 0000-Apr 30 0400	4.0	8
...	May 10 0600-May 10 1200	6.0	8
...	Jun 21 1400-Jun 21 2000	6.0	8
...	Jul 22 1400-Jul 22 1800	4.0	8
Sep 14 0954	Sep 14 1200-Sep 14 1800	6.0	8
...	Sep 22 0000-Sep 22 0800	8.0	8
...	Oct 18 1200-Oct 18 1600	4.0	8
Nov 12 1025	Nov 13 0800-Nov 13 1400	6.0	8
...	Dec 12 1000-Dec 12 1400	4.0	8
1977			
...	Jan 7 0800-Jan 7 1200	4.0	8
Jan 18 0422	Jan 18 2000-Jan 19 0200	6.0	8
Jan 30 0012	Jan 30 1000-Jan 31 0000	14.0	8
...	May 2 2200-May 3 0400	6.0	8He
...	Jun 2 2000-Jun 3 0200	6.0	8
...	Jul 11 1200-Jul 11 1800	6.0	8
...	Aug 31 0800-Aug 31 1800	10.0	8
Sep 2 1751	Sep 4 0000-Sep 4 0600	6.0	8
...	Sep 15 2000-Sep 16 0200	6.0	8
Sep 21 2044	Sep 22 1800-Sep 22 2200	4.0	8HeF
	Sep 23 0400-Sep 23 0800	4.0	8
Oct 12 0151	Oct 12 1400-Oct 12 2000	6.0	8K
...	Oct 31 0800-Oct 31 1400	6.0	8
...	Dec 18 2200-Dec 19 0200	4.0	8
...	Dec 22 0400-Dec 22 1200	8.0	8
1978			
Jan 3 2042	Jan 4 1200-Jan 4 1800	6.0	8*CF
	Jan 5 1000-Jan 5 2000	10.0	8CHe
Jan 5 1628	Jan 6 0200-Jan 6 0600	4.0	8
	Jan 7 0800-Jan 7 1600	8.0	8
...	Jan 19 0000-Jan 19 0600	6.0	8
...	Jan 19 2200-Jan 20 0200	4.0	8
...	Feb 22 1400-Feb 22 1800	4.0	8*
Feb 22 1800	Feb 24 1600-Feb 25 0200	10.0	8
...	Mar 5 0200-Mar 5 1400	12.0	8He
...	Mar 5 1800-Mar 6 0000	6.0	8F
...	Mar 7 1400-Mar 7 1800	4.0	8
Mar 8 1439	Mar 9 0000-Mar 9 0600	6.0	8He
	Mar 9 1000-Mar 9 1600	6.0	8
...	Apr 1 0000-Apr 1 0400	4.0	8
Apr 2 2057	Apr 4 0000-Apr 4 0400	4.0	8C
Apr 13 1925	Apr 14 1600-Apr 14 2200	6.0	8He
Apr 17 2345	Apr 18 1200-Apr 18 2000	8.0	8*FHe
May 1 0828	May 1 1800-May 1 2000	2.0	8*F
May 7 2155	May 9 1600-May 9 1800	2.0	8*He
May 10 2005	May 11 0200-May 11 0600	4.0	8
...	May 13 0400-May 13 0800	4.0	8
...	May 13 1400-May 13 1800	4.0	8
...	May 20 1200-May 20 1600	4.0	8
May 21 0241	May 22 0400-May 22 0800	4.0	8
	May 22 1200-May 23 1400	26.0	8He
Jun 2 0913	Jun 2 2200-Jun 3 0000	2.0	8*FHe
	Jun 3 2200-Jun 4 0200	4.0	8F
Jun 4 1211	Jun 5 0600-Jun 5 1000	4.0	8C
	Jun 6 1000-Jun 6 1400	4.0	8
...	Jun 6 2000-Jun 7 0600	10.0	8
...	Jun 17 0400-Jun 17 0800	4.0	8
Jun 25 0825	Jun 26 1600-Jun 27 0600	14.0	8*F
...	Jul 2 1800-Jul 2 2200	4.0	8
...	Jul 10 1000-Jul 10 1400	4.0	8
...	Jul 12 0600-Jul 12 1000	4.0	8
...	Jul 16 0400-Jul 16 0800	4.0	8He
...	Jul 16 1600-Jul 16 2000	4.0	8
...	Jul 24 1600-Jul 24 2200	6.0	8
...	Aug 2 2200-Aug 3 0200	4.0	8
...	Aug 3 2000-Aug 4 0000	4.0	8
...	Aug 8 1600-Aug 9 0200	10.0	8
...	Sep 9 1200-Sep 9 2000	8.0	8
Sep 10 0105	Sep 10 0400-Sep 10 1000	6.0	8HeG
	Sep 10 0900-Sep 10 1400	5.0	3HeG
Sep 29 0301	Sep 29 0915-Sep 29 2245	13.5	3*CHeGM
	Sep 30 0600-Sep 30 1130	5.5	3He
	Sep 30 1545-Sep 30 2145	6.0	3He
Oct 4 0047	Oct 4 0600-Oct 5 0730	25.5	3*
	Oct 4 1200-Oct 4 1800	6.0	8*
	Oct 4 2200-Oct 5 0400	6.0	8
...	Oct 7 1230-Oct 7 1800	5.5	3
...	Oct 7 2145-Oct 8 0745	10.0	3
...	Oct 8 0200-Oct 8 0400	2.0	8*
...	Oct 8 1430-Oct 9 0000	9.5	3
...	Oct 11 2145-Oct 12 0445	7.0	3
Oct 17 0430	Oct 17 0600-Oct 17 1000	4.0	8
	Oct 18 2000-Oct 19 0400	8.0	8
...	Oct 21 0400-Oct 21 0800	4.0	8
	Oct 21 0715-Oct 21 1230	5.25	3
Oct 29 1116	Oct 30 0200-Oct 30 0600	4.0	8CGM
...	Nov 1 2200-Nov 2 0400	6.0	8
...	Nov 10 2000-Nov 10 2200	2.0	8*F

TABLE 2—*Continued*

Shock	Bi Interval	Duration	S/C
Nov 12 0100	Nov 12 1800-Nov 13 0200	8.0	8*HeGM
	Nov 12 1815-Nov 13 0130	7.25	3*HeGM
	Nov 13 1415-Nov 13 1615	2.0	3*M
...	Nov 14 1800-Nov 14 2200	4.0	8
...	Nov 16 1045-Nov 16 2115	10.5	3
...	Nov 23 0000-Nov 23 0400	4.0	8
...	Dec 3 0430-Dec 3 0845	4.25	3
...	Dec 3 1945-Dec 4 0300	7.25	3
...	Dec 4 1100-Dec 4 1500	4.0	3
Dec 14 0127	Dec 15 2315-Dec 16 0600	6.75	3M
...	Dec 17 0130-Dec 17 0730	6.0	3He
...	Dec 24 2000-Dec 25 0600	10.0	8
1979			
...	Jan 1 1600-Jan 1 2200	6.0	8He
Jan 2 2100	Jan 2 2000-Jan 3 0000	4.0	8
	Jan 2 2300-Jan 3 2230	23.5	3*HeM
	Jan 3 0400-Jan 3 2200	18.0	8HeM
	Jan 4 0415-Jan 4 1345	9.5	3M
	Jan 4 1730-Jan 4 2300	5.5	3M
	Jan 4 2000-Jan 5 0000	4.0	8
Jan 6 0032	Jan 6 0345-Jan 6 2145	18.0	3
	Jan 6 2200-Jan 7 0400	6.0	8M
	Jan 7 0215-Jan 7 0630	4.25	3GM
	Jan 7 1330-Jan 7 2230	9.0	3GM
...	Jan 8 0415-Jan 8 1345	9.5	3GM
...	Jan 15 1000-Jan 15 1400	4.0	8
Jan 22 1900	Jan 23 1745-Jan 24 0230	8.75	3G
Jan 25 0045	Jan 25 0115-Jan 25 0800	6.75	3G
Feb 11 0148	Feb 11 0430-Feb 11 1100	6.5	3
	Feb 12 2000-Feb 13 0400	8.0	8M
	Feb 12 2215-Feb 13 0415	6.0	3M
...	Feb 13 1015-Feb 13 1615	6.0	3*M
...	Feb 14 1015-Feb 14 2015	10.0	3M
Feb 18 0304	Feb 18 0600-Feb 18 1645	10.8	3*
...	Feb 20 1600-Feb 20 2000	4.0	8
Feb 21 0302	Feb 21 1945-Feb 22 0700	11.3	3He
...	Feb 23 0900-Feb 23 1815	9.25	3GMF
...	Feb 23 2215-Feb 24 0645	8.5	3F
Feb 28 1200	Mar 1 1900-Mar 1 2315	4.25	3
...	Mar 3 2215-Mar 4 0215	4.0	3
Mar 4 0445	Mar 4 1415-Mar 4 1945	5.5	3
Mar 6 0818	Mar 7 2200-Mar 8 0200	4.0	8
...	Mar 8 1730-Mar 9 0100	7.5	3
Mar 9 0808	Mar 9 1800-Mar 10 0800	14.0	3*HeG
	Mar 10 0400-Mar 10 0800	4.0	8*HeG
...	Mar 11 1400-Mar 12 1200	22.0	3*
...	Mar 19 1000-Mar 19 1800	8.0	8He
Mar 21 1251	Mar 21 1800-Mar 22 0000	6.0	8
	Mar 21 2015-Mar 22 0515	9.0	3
...	Mar 27 1745-Mar 27 2230	4.75	3
Mar 28 0827	Mar 30 0245-Mar 30 1400	11.3	3HeF
...	Mar 31 1730-Apr 1 0030	7.0	3
Apr 1 2150	Apr 3 0215-Apr 3 0915	7.0	3M
	Apr 3 0600-Apr 3 1000	4.0	8M
Apr 3 1001	Apr 3 1945-Apr 4 0015	4.5	3*CG
	Apr 3 2200-Apr 4 0400	6.0	8*CG
Apr. 5 0156	Apr 6 0145-Apr 6 1500	13.3	3*GM
	Apr 7 0245-Apr 7 1000	7.25	3*
...	Apr 8 1515-Apr 9 0445	13.5	3*G
...	Apr 9 2015-Apr 10 0115	5.0	3*
...	Apr 10 1015-Apr 10 2000	9.75	3
...	Apr 14 2215-Apr 15 0215	4.0	3
Apr 24 2358	Apr 25 2345-Apr 26 1445	15.0	3*F
	Apr 26 0600-Apr 26 1000	4.0	8
...	May 10 0015-May 10 0615	6.0	3*
...	May 10 1000-May 10 1400	4.0	8
...	May 13 1215-May 13 1730	5.25	3
...	May 14 1230-May 14 1900	6.5	3
...	May 19 1600-May 19 2000	4.0	8
May 29 1851	May 30 0215-May 31 1300	34.8	3*GM
	May 30 1000-May 31 1400	28.0	8*GM
...	Jun 3 0200-Jun 3 1000	8.0	8*
	Jun 3 0230-Jun 3 1100	8.5	3
...	Jun 5 1100-Jun 5 2015	9.25	3
...	Jun 6 0300-Jun 6 1045	7.75	3
...	Jun 6 1615-Jun 6 1815	2.0	3*G
...	Jun 16 0800-Jun 16 1600	8.0	8
...	Jun 17 1400-Jun 17 2200	8.0	8
...	Jun 18 0800-Jun 18 1200	4.0	8
...	Jun 25 2330-Jun 26 0830	9.0	3
...	Jun 27 2000-Jun 28 0000	4.0	8
...	Jun 29 1200-Jun 29 1800	6.0	8
...	Jul 4 2000-Jul 5 0215	6.25	3
Jul 6 1930	Jul 8 0530-Jul 8 1015	4.75	3*F
...	Jul 10 0600-Jul 10 0800	2.0	8*
Jul 12 1240	Jul 13 0115-Jul 13 0515	4.0	3
	Jul 13 2200-Jul 14 0200	4.0	8
...	Jul 26 0600-Jul 26 1200	6.0	8
Jul 26 1833	Jul 28 0015-Jul 28 0445	4.5	3
...	Aug 1 0415-Aug 1 0815	4.0	3
...	Aug 4 1000-Aug 4 1400	4.0	8
...	Aug 6 1200-Aug 6 1600	4.0	8
...	Aug 7 2300-Aug 8 0330	4.5	3
...	Aug 9 1445-Aug 9 1945	5.0	3
Aug 11 1812	Aug 12 0845-Aug 12 1845	10.0	3
Aug 13 0611	Aug 14 0715-Aug 14 1345	6.5	3
	Aug 14 1700-Aug 14 2145	4.75	3
...	Aug 15 1800-Aug 15 2330	5.5	3
...	Aug 16 2215-Aug 17 0400	5.75	3
...	Aug 17 0600-Aug 17 1200	6.0	8
...	Aug 17 1700-Aug 18 0315	10.3	3
	Aug 17 2000-Aug 18 0000	4.0	8
...	Aug 23 1330-Aug 23 1915	5.75	3
Aug 29 0459	Aug 30 0000-Aug 30 1200	12.0	3*G
Aug 31 0510	Sep 1 1600-Sep 1 2000	4.0	8
...	Sep 9 0815-Sep 9 1945	11.5	3M
	Sep 9 1800-Sep 9 2200	4.0	8M
...	Sep 13 0930-Sep 13 1345	4.25	3
...	Sep 13 1815-Sep 13 2330	5.25	3
Sep 17 0448	Sep 18 0815-Sep 18 1015	2.0	3*CG
	Sep 18 1415-Sep 18 2145	7.5	3*CGM
	Sep 19 1415-Sep 19 1615	2.0	3*CHe
...	Sep 20 0100-Sep 20 0615	5.25	3
...	Sep 26 1115-Sep 26 2000	8.75	3
	Sep 26 1200-Sep 26 1600	4.0	8
...	Sep 27 1600-Sep 27 2015	4.25	3
...	Sep 28 0800-Sep 28 1215	4.25	3
...	Sep 29 0600-Sep 29 1630	10.5	3
...	Oct 3 0200-Oct 3 1200	10.0	8
...	Oct 5 0200-Oct 5 1000	8.0	8G
Oct 6 1120	Oct 7 2000-Oct 8 0200	6.0	8*F
	Oct 7 2215-Oct 8 0330	6.25	3*F
...	Nov 5 0545-Nov 5 1815	12.5	3
Nov 7 1347	Nov 7 1445-Nov 7 2015	5.5	3
Nov 11 0225	Nov 11 2230-Nov 12 0400	5.5	3He
	Nov 12 2015-Nov 13 0715	11.0	3G
	Nov 12 2200-Nov 13 0400	6.0	8G
...	Nov 14 0715-Nov 14 1515	8.0	3
Nov 18 0139	Nov 18 0130-Nov 18 0530	4.0	3
	Nov 18 0930-Nov 18 2245	13.3	3
	Nov 19 1745-Nov 20 0015	6.5	3
...	Nov 21 0945-Nov 21 1615	6.5	3
...	Nov 22 1515-Nov 23 0015	9.0	3
...	Nov 23 1300-Nov 23 1715	4.25	3G
...	Nov 24 2200-Nov 25 0400	6.0	8
...	Nov 25 1000-Nov 25 1800	8.0	8M
...	Nov 25 2200-Nov 26 0200	4.0	8M
	Nov 26 0000-Nov 26 1000	10.0	3M
...	Nov 28 0800-Nov 28 1200	4.0	8
...	Nov 29 0600-Nov 29 2045	14.8	3*
	Nov 29 0800-Nov 29 1200	4.0	8
...	Dec 20 1800-Dec 20 2200	4.0	8
...	Dec 21 1000-Dec 21 1400	4.0	8
...	Dec 22 1115-Dec 22 1745	6.5	3
...	Dec 23 0600-Dec 23 1315	7.25	3
	Dec 23 1400-Dec 24 0400	14.0	8
	Dec 24 0200-Dec 24 1145	9.75	3
...	Dec 25 0215-Dec 25 0700	4.75	3
...	Dec 26 1815-Dec 27 0000	5.75	3

TABLE 2—*Continued*

Shock	Bi Interval	Duration	S/C
...	Dec 29 1100-Dec 29 1500	4.0	3
Dec 30 1000	Dec 30 0515-Dec 30 1200	6.75	3
	Dec 31 1715-Jan 1 0800	14.8	3G
1980			
	Jan 1 0000-Jan 1 1000	10.0	8G
Jan 13 0510	Jan 13 1700-Jan 14 0130	8.5	3GM
	Jan 13 2000-Jan 14 0000	4.0	8GM
	Jan 14 0600-Jan 14 1000	4.0	8GM
Jan 25 1109	Jan 27 0530-Jan 27 0945	4.25	3*
	Jan 27 0600-Jan 27 1000	4.0	8
	Jan 27 1330-Jan 27 1530	2.0	3*
...	Feb 5 0345-Feb 5 0845	5.0	3
Feb 9 0338	Feb 9 0800-Feb 9 1800	10.0	8
	Feb 10 2300-Feb 11 0515	6.25	3
...	Feb 11 1900-Feb 12 0115	6.25	3
...	Feb 12 2000-Feb 13 0200	6.0	8
Feb 14 0309	Feb 14 1445-Feb 15 0045	10.0	3*G
Feb 15 1235	Feb 16 1245-Feb 16 1715	4.5	3CGM
...	Feb 17 1730-Feb 17 1930	2.0	3*G
...	Feb 17 2200-Feb 18 0200	4.0	3G
...	Feb 18 1600-Feb 18 2200	6.0	8
	Feb 18 1715-Feb 19 0030	7.25	3
...	Feb 20 0600-Feb 20 1000	4.0	8
Feb 25 1429	Feb 25 1600-Feb 25 2200	6.0	8
...	Mar 2 1800-Mar 2 2200	4.0	8
...	Mar 9 0800-Mar 9 1400	6.0	8
...	Mar 30 0900-Mar 30 1915	10.3	3
Mar 30 2354	Apr 1 0130-Apr 1 2300	21.5	3*GM
	Apr 1 0200-Apr 2 1000	32.0	8*GMF
...	Apr 2 0700-Apr 2 1745	10.8	3*GF
Apr 2 2110	Apr 3 0800-Apr 3 1600	8.0	8
	Apr 4 0730-Apr 4 1215	4.75	3
...	Apr 8 1600-Apr 8 2130	5.5	3
Apr 9 0508	Apr 9 1315-Apr 10 0115	12.0	3G
Apr 10 1710	Apr 10 2200-Apr 11 1400	16.0	8G
	Apr 12 1400-Apr 12 1800	4.0	8
...	Apr 13 0800-Apr 13 1200	4.0	8
...	Apr 15 0600-Apr 15 1200	6.0	8
...	Apr 19 0115-Apr 19 1215	11.0	3
...	Apr 20 0100-Apr 20 0800	7.0	3
Apr 25 0000	Apr 25 0200-Apr 25 0800	6.0	8
May 5 0700	May 5 1515-May 5 2030	5.25	3
...	May 10 1600-May 10 2200	6.0	8
...	May 11 0645-May 11 1345	7.0	3
...	May 21 2200-May 22 0200	4.0	8G
...	May 22 0600-May 22 1200	6.0	8
...	May 23 0600-May 23 1200	6.0	8
May 29 1832	May 31 0215-May 31 1615	14.0	3G
May 31 2137	Jun 1 1015-Jun 1 1645	6.5	3
...	Jun 3 0800-Jun 3 1315	5.25	3
Jun 4 0300	Jun 4 0545-Jun 4 1930	13.8	3
...	Jun 9 2215-Jun 10 0415	6.0	3
...	Jun 13 2200-Jun 14 0600	8.0	8
...	Jun 14 1000-Jun 14 1600	6.0	8
...	Jun 15 0800-Jun 15 1200	4.0	8
...	Jun 17 0200-Jun 17 0600	4.0	8
...	Jun 18 0215-Jun 18 0745	5.5	3
...	Jun 20 2145-Jun 21 0430	6.75	3
...	Jun 22 0200-Jun 22 0745	5.75	3
Jun 24 0248	Jun 24 0800-Jun 24 1400	6.0	8
	Jun 25 1400-Jun 25 2000	6.0	8F
...	Jun 26 2130-Jun 27 0345	6.25	3G
...	Jun 27 1430-Jun 27 1945	5.25	3
...	Jun 29 2230-Jun 30 0700	8.5	3
	Jun 30 0000-Jun 30 0600	6.0	8
...	Jul 6 2200-Jul 7 0200	4.0	8
...	Jul 7 0600-Jul 7 1000	4.0	8
...	Jul 10 0400-Jul 10 1000	6.0	8
...	Jul 15 1400-Jul 15 1800	4.0	3
...	Jul 22 2130-Jul 23 0300	5.5	3
...	Jul 23 1600-Jul 24 0000	8.0	8
Jul 27 0157	Jul 29 0115-Jul 29 0630	5.25	3G
...	Jul 30 0015-Jul 30 0515	5.0	3G
...	Aug 8 1245-Aug 8 1700	4.25	3
...	Aug 9 1245-Aug 9 1815	5.5	3
Aug 11 1656	Aug 13 0200-Aug 13 0600	4.0	8
...	Aug 13 1730-Aug 14 0330	10.0	3M
	Aug 14 0000-Aug 14 0400	4.0	8M
...	Aug 19 0000-Aug 19 0445	4.75	3
Aug 19 1024	Aug 19 1430-Aug 20 1430	24.0	3*M
	Aug 20 0400-Aug 20 1000	6.0	8M
	Aug 20 1800-Aug 21 0200	8.0	3M
...	Aug 22 1630-Aug 23 0315	10.8	3
...	Aug 31 1600-Sep 1 0000	8.0	8
Sep 3 1336	Sep 4 0015-Sep 4 1015	10.0	3*G
...	Sep 7 0730-Sep 7 1615	8.75	3
...	Sep 7 2215-Sep 8 0645	8.5	3
...	Sep 9 1930-Sep 10 0045	5.25	3
...	Sep 10 1645-Sep 10 2230	5.75	3
...	Sep 11 1600-Sep 11 2000	4.0	8G
...	Sep 12 2000-Sep 13 1000	14.0	8GM
Sep 20 0139	Sep 19 2230-Sep 20 0500	6.5	3
	Sep 21 1000-Sep 21 1400	4.0	8
...	Oct 4 0315-Oct 4 1030	7.25	3
...	Oct 4 2045-Oct 5 0430	7.75	3
...	Oct 5 1830-Oct 6 0215	7.75	3
...	Oct 6 1130-Oct 7 0630	19.0	3*G
	Oct 6 1200-Oct 6 1800	6.0	8G
	Oct 6 2200-Oct 7 0200	4.0	8G
...	Oct 7 1130-Oct 7 2130	10.0	3
	Oct 7 1400-Oct 7 2000	6.0	8
...	Oct 8 0230-Oct 8 0830	6.0	3
Oct 14 1953	Oct 15 0715-Oct 15 1200	4.75	3*GM
	Oct 15 0800-Oct 15 2000	12.0	8*GM
	Oct 15 1515-Oct 15 2130	6.25	3*GM
	Oct 16 0800-Oct 16 1200	4.0	8
...	Oct 27 0800-Oct 27 1200	4.0	8F
...	Nov 3 1515-Nov 3 2115	6.0	3
Nov 9 1122	Nov 9 1330-Nov 10 0645	17.3	3*
	Nov 9 1400-Nov 9 2200	8.0	8
	Nov 10 1400-Nov 11 0000	10.0	8*F
Nov 14 1153	Nov 16 0045-Nov 16 0545	5.0	3
...	Nov 18 0415-Nov 18 1330	9.25	3
...	Nov 19 1600-Nov 19 2030	4.5	3
...	Nov 19 2345-Nov 20 0615	6.5	3
...	Nov 22 0100-Nov 22 0830	7.5	3
...	Nov 22 1745-Nov 23 0000	6.25	3
...	Nov 23 1200-Nov 23 1800	6.0	8
...	Nov 29 0730-Nov 29 0930	2.0	3*G
...	Nov 29 1330-Nov 30 0030	11.0	3*GF
...	Dec 1 0330-Dec 1 1800	14.5	3*G
...	Dec 4 1730-Dec 5 0715	13.75	3
...	Dec 7 2015-Dec 8 0045	4.5	3
...	Dec 10 0400-Dec 10 1000	6.0	8
Dec 11 1009	Dec 11 2330-Dec 12 0700	7.5	3CGM
...	Dec 17 1745-Dec 17 2200	4.25	3
	Dec 17 2200-Dec 18 0200	4.0	8
...	Dec 18 1800-Dec 19 0000	6.0	8
...	Dec 21 1200-Dec 21 2000	8.0	8F
	Dec 21 1330-Dec 21 1530	2.0	3*F
Dec 25 0552	Dec 27 0230-Dec 27 1800	15.5	3*G
...	Dec 28 0930-Dec 28 1130	2.0	3*G
Dec 30 0738	Dec 31 0800-Dec 31 1200	4.0	8
	Dec 31 1130-Dec 31 1530	4.0	3
1981			
	Jan 1 0000-Jan 1 0400	4.0	8
...	Jan 25 1400-Jan 25 1800	4.0	8
Jan 29 0646	Jan 29 2130-Jan 30 0630	9.0	3*G
	Jan 30 0000-Jan 30 1000	10.0	8G
...	Jan 31 1530-Jan 31 2000	4.5	3G
...	Feb 1 2200-Feb 2 0215	4.25	3F
...	Feb 6 0200-Feb 6 0600	4.0	8
Feb 6 0847	Feb 6 1745-Feb 6 2300	5.25	3*CGM
	Feb 6 1800-Feb 7 0000	6.0	8CGM
	Feb 7 0530-Feb 7 1800	12.5	3CGM
	Feb 7 0600-Feb 7 1800	12.0	8CGM
Feb 8 1345	Feb 9 0200-Feb 9 0600	4.0	8G
...	Feb 20 1000-Feb 21 0000	14.0	8*GM

TABLE 2—*Continued*

Shock	Bi Interval	Duration	S/C
	Feb 20 1330-Feb 21 0200	12.5	3*GM
...	Feb 23 0515-Feb 23 1000	4.75	3
...	Feb 28 1000-Feb 28 1400	4.0	3
Mar 1 0737	Mar 1 1115-Mar 1 2115	10.0	3*
Mar 2 0654	Mar 2 1930-Mar 3 0915	13.8	3*
	Mar 3 1600-Mar 4 0000	8.0	8
Mar 7 0153	Mar 7 1730-Mar 7 2215	4.75	3*M
	Mar 7 1800-Mar 8 0000	6.0	8M
...	Mar 18 1800-Mar 19 0815	14.3	3
...	Mar 19 1400-Mar 19 2000	6.0	8
...	Mar 20 2000-Mar 21 0315	7.25	3
...	Mar 21 0645-Mar 21 1345	7.0	3
...	Mar 23 1545-Mar 23 2215	6.5	3
...	Mar 24 0330-Mar 24 0930	6.0	3
...	Mar 31 1800-Apr 1 0400	10.0	8
...	Apr 6 1100-Apr 6 2015	9.25	3
...	Apr 7 0615-Apr 7 1300	6.75	3
Apr 7 1954	Apr 8 1800-Apr 9 0100	7.0	3M
...	Apr 9 2030-Apr 10 0100	4.5	3
Apr 11 1339	Apr 11 1800-Apr 12 0000	6.0	8
Apr 12 2120	Apr 13 2130-Apr 14 1300	15.5	3*GM
	Apr 13 2200-Apr 14 0000	2.0	8*GM
Apr 18 1503	Apr 19 1130-Apr 20 0245	15.3	3*G
...	Apr 22 0015-Apr 22 0800	7.75	3
...	Apr 24 1000-Apr 24 1600	6.0	8
Apr 26 0813	Apr 26 1530-Apr 26 1730	2.0	3*
May 1 0745	May 2 1115-May 3 0730	20.3	3
...	May 3 1415-May 4 0030	10.3	3
...	May 4 0500-May 4 0900	4.0	3
...	May 4 1845-May 5 2015	25.5	3
...	May 9 0800-May 9 1400	6.0	8
...	May 13 0830-May 13 2000	11.5	3*GM
May 15 0252	May 15 0530-May 15 1945	14.3	3*G
May 17 2302	May 18 1200-May 18 1800	6.0	8G
	May 18 1330-May 18 1730	4.0	3*G
...	May 24 2330-May 25 0800	8.5	3*M
...	May 25 1545-May 26 0900	17.3	3*GM
...	May 26 1345-May 26 2015	6.5	3GM
...	May 27 0115-May 27 1530	14.3	3G
...	Jun 1 2130-Jun 2 0300	5.5	3
Jun 7 0823	Jun 7 2015-Jun 8 0100	4.75	3G
	Jun 8 0700-Jun 8 2030	13.5	3G
...	Jun 14 1530-Jun 14 2230	7.0	3*M
	Jun 14 2000-Jun 15 0000	4.0	8M
...	Jun 16 0815-Jun 16 1245	4.5	3
...	Jun 17 1730-Jun 17 2330	6.0	3*
...	Jun 27 0045-Jun 27 0915	8.5	3
Jun 29 0610	Jun 30 0730-Jun 30 1245	5.25	3
...	Jul 9 1830-Jul 9 2345	5.25	3
...	Jul 10 2145-Jul 11 0930	11.8	3
...	Jul 14 2130-Jul 15 0145	4.25	3
...	Jul 16 0000-Jul 16 0830	8.5	3
...	Jul 16 1600-Jul 16 2000	4.0	3
Jul 17 0802	Jul 18 0800-Jul 18 1000	2.0	3*GM
Jul 23 0646	Jul 23 1400-Jul 23 2200	8.0	8*GF
	Jul 23 1400-Jul 24 0745	17.8	3*GF
Jul 25 0514	Jul 26 0000-Jul 26 1215	12.3	3*GM
	Jul 26 1645-Jul 27 1815	25.5	3*GM
...	Jul 30 2215-Jul 31 0600	7.75	3
...	Aug 5 1600-Aug 6 0200	10.0	8
...	Aug 6 2200-Aug 7 0400	6.0	8
...	Aug 9 0215-Aug 9 0715	5.0	3F
...	Aug 15 0200-Aug 15 0800	6.0	8
...	Aug 16 2000-Aug 17 0200	6.0	8
...	Aug 19 1400-Aug 19 2000	6.0	8
...	Aug 29 1615-Aug 30 0130	9.25	3
Aug 30 2222	Aug 31 1200-Sep 1 1015	22.3	3
...	Sep 2 1415-Sep 2 2300	8.75	3
...	Sep 11 1000-Sep 11 1715	7.25	3G
Sep 18 1912	Sep 19 1400-Sep 19 1800	4.0	3CM
	Sep 19 2245-Sep 20 0530	6.75	3
...	Sep 22 1800-Sep 23 0000	6.0	3*G
	Sep 23 0000-Sep 23 0600	6.0	8G
...	Sep 23 1400-Sep 23 2130	7.5	3G
	Sep 23 1800-Sep 24 0000	6.0	8G
...	Sep 28 2115-Sep 29 0300	5.75	3
...	Sep 29 1515-Sep 29 2245	7.5	3
...	Sep 30 1145-Sep 30 2000	8.25	3
Oct 2 2022	Oct 3 2000-Oct 4 0000	4.0	8F
...	Oct 8 0800-Oct 8 1400	6.0	8
Oct 10 1434	Oct 12 1000-Oct 12 1730	7.5	3*F
...	Oct 18 0000-Oct 18 0600	6.0	8
	Oct 18 0045-Oct 18 0800	7.25	3*
...	Oct 20 0845-Oct 20 1400	7.25	3*
...	Oct 21 0400-Oct 21 0800	4.0	8*
Oct 22 0525	Oct 22 1945-Oct 23 0100	5.25	3
	Oct 23 1215-Oct 24 0115	13.0	3
...	Oct 31 1000-Oct 31 1400	4.0	8
...	Nov 5 0745-Nov 5 1345	6.0	3
...	Nov 6 2100-Nov 7 1100	14.0	3*
...	Nov 7 1600-Nov 8 0030	8.5	3*
...	Nov 8 1600-Nov 8 2200	6.0	8
	Nov 8 1900-Nov 9 0400	9.0	3
...	Nov 10 1600-Nov 10 2000	4.0	8
Nov 11 1238	Nov 12 2000-Nov 13 0830	12.5	3*GF
...	Nov 22 1600-Nov 22 1800	2.0	3*
...	Nov 22 2200-Nov 23 0400	6.0	8
Dec 8 1400	Dec 9 2200-Dec 10 0200	4.0	8G
	Dec 9 2200-Dec 10 0200	4.0	3*G
Dec 12 0144	Dec 13 1000-Dec 13 1530	5.5	3G
	Dec 14 1000-Dec 14 1200	2.0	3*
1982			
...	Jan 1 0200-Jan 1 0845	6.75	3G
...	Jan 10 0600-Jan 10 1600	10.0	8
	Jan 10 1000-Jan 10 1200	4.0	3
	Jan 10 1600-Jan 10 2245	6.75	3
Jan 29 1745	Jan 31 1400-Feb 1 0100	11.0	3*GMF
...	Feb 5 0415-Feb 5 1730	13.3	3*GM
...	Feb 9 0745-Feb 9 1515	7.5	3GM
	Feb 9 1400-Feb 9 1600	2.0	8*GM
Feb 11 1313	Feb 12 1130-Feb 12 2000	8.5	3*CGMF
	Feb 13 0030-Feb 13 0815	7.75	3CGM
...	Feb 14 2030-Feb 15 0530	9.0	3G
...	Feb 20 1400-Feb 20 2000	6.0	8
Feb 21 0727	Feb 21 0445-Feb 21 1145	7.0	3
Mar 1 1138	Mar 2 0400-Mar 2 0930	5.5	3
...	Mar 12 1615-Mar 12 2145	5.5	3
...	Mar 17 0300-Mar 17 1000	7.0	3G
...	Mar 21 0500-Mar 21 1615	11.3	3*
...	Mar 22 1200-Mar 22 1600	4.0	8
...	Mar 23 2200-Mar 24 0315	5.25	3
...	Mar 28 0500-Mar 28 0900	4.0	3
...	Apr 4 0415-Apr 4 0930	5.25	3
...	Apr 10 2315-Apr 11 0830	9.25	3
...	Apr 12 0400-Apr 12 1000	6.0	8
...	Apr 13 2100-Apr 14 0545	8.75	3
...	Apr 14 1800-Apr 14 2300	5.0	3
Apr 24 2016	Apr 26 0245-Apr 26 1230	9.75	3GMF
...	Apr 28 0145-Apr 28 0800	6.25	3
...	May 7 2315-May 8 0645	7.5	3
...	May 11 1300-May 11 1700	4.0	3
...	May 14 1900-May 14 2100	2.0	3*
...	May 31 0200-May 31 0600	4.0	8
...	May 31 2045-Jun 1 0100	4.25	3
...	Jun 1 1000-Jun 1 1400	4.0	8
	Jun 1 1000-Jun 1 1615	6.25	3
...	Jun 2 0800-Jun 2 1230	4.5	3
Jun 6 0244	Jun 7 1300-Jun 7 1830	5.5	3*F
Jun 9 0040	Jun 9 1300-Jun 9 2000	7.0	3*G
Jun 12 1443	Jun 13 1300-Jun 13 2145	8.75	3G
	Jun 13 1400-Jun 14 0200	12.0	8G
...	Jun 17 0330-Jun 17 0830	5.0	3
...	Jun 21 1500-Jun 21 1700	2.0	3*
...	Jun 22 0215-Jun 22 1300	10.8	3
...	Jun 23 1000-Jun 23 1415	4.25	3G
...	Jul 7 1400-Jul 7 1800	4.0	8
...	Jul 8 1800-Jul 8 2200	4.0	8
Jul 13 1617	Jul 14 0000-Jul 14 0600	6.0	8G
	Jul 14 0615-Jul 15 1130	29.25	3*G

TABLE 2—*Continued*

Shock	Bi Interval	Duration	S/C
Jul 16 1519	Jul 17 0100-Jul 17 0615	5.25	3*G
	Jul 17 1100-Jul 17 1530	4.5	3*
	Jul 18 1445-Jul 18 2115	6.5	3G
...	Jul 20 0100-Jul 20 0500	4.0	3*
...	Jul 21 0800-Jul 21 1400	6.0	8
...	Jul 22 0630-Jul 22 1130	5.0	3
Aug 6 1836	Aug 6 2200-Aug 7 0200	4.0	8G
	Aug 7 0045-Aug 7 0800	7.25	3G
...	Aug 15 1800-Aug 15 2200	4.0	8
...	Aug 28 0900-Aug 28 1100	2.0	3*
Sep 5 2250	Sep 6 1900-Sep 7 0015	5.25	3GF
	Sep 7 1545-Sep 7 2100	5.25	3G
...	Sep 12 2000-Sep 13 0130	5.5	3
...	Sep 15 1430-Sep 15 2130	7.0	3
...	Sep 16 1830-Sep 16 2245	4.25	3
Sep 21 0339	Sep 21 1415-Sep 22 0515	10.0	3*G
	Sep 21 1600-Sep 22 0600	14.0	8*G
	Sep 22 1600-Sep 22 2000	4.0	8*G
	Sep 22 1600-Sep 22 2115	5.25	3*G
...	Sep 23 1230-Sep 23 1715	4.75	3
	Sep 23 1400-Sep 23 1800	4.0	8
...	Sep 24 0000-Sep 24 0400	4.0	8
...	Sep 24 1230-Sep 24 1915	6.75	3
...	Sep 25 0900-Sep 25 1645	7.75	3C
...	Oct 4 0600-Oct 4 1200	6.0	8
	Oct 4 1230-Oct 4 1700	4.5	3
...	Oct 5 1615-Oct 5 2230	6.25	3
...	Oct 6 1130-Oct 6 1600	4.5	3
...	Oct 22 0000-Oct 22 0400	4.0	8
...	Oct 28 0400-Oct 28 1400	10.0	8
...	Oct 30 0800-Oct 30 1200	4.0	8
Oct 31 1338	Nov 1 0100-Nov 1 1545	14.8	3*
	Nov 1 0200-Nov 1 0600	4.0	8
	Nov 2 1400-Nov 3 0000	10.0	8
	Nov 2 1530-Nov 3 0300	11.5	3
...	Nov 4 0000-Nov 4 0800	8.0	3
	Nov 4 0600-Nov 4 1200	6.0	8
...	Nov 8 2245-Nov 9 0245	4.0	3
...	Nov 21 1100-Nov 21 1945	8.75	3
...	Nov 22 0400-Nov 22 1000	6.0	8*
...	Nov 29 0800-Nov 29 1400	6.0	8
...	Dec 5 0700-Dec 5 1215	5.25	3*
...	Dec 6 0645-Dec 6 1200	5.25	3
Dec 7 0329	Dec 8 0100-Dec 8 0615	5.25	3
...	Dec 15 0730-Dec 15 1845	11.3	3*C
...	Dec 16 0245-Dec 16 0830	5.75	3C
...	Dec 16 1215-Dec 17 0330	15.3	3*C
Dec 17 0806	Dec 18 1530-Dec 19 0300	11.5	3*
	Dec 18 2000-Dec 19 0400	8.0	8
	Dec 19 0800-Dec 19 1600	8.0	8
	Dec 19 1130-Dec 19 1700	5.5	3*
...	Dec 20 0830-Dec 20 1415	5.75	3*
	Dec 20 1200-Dec 20 1400	2.0	8*
...	Dec 21 0700-Dec 21 1630	9.5	3
1983			
...	Jan 2 1800-Jan 3 0000	6.0	8
Jan 11 2309	Jan 12 2000-Jan 13 0400	8.0	8
...	Jan 14 2000-Jan 15 0000	4.0	8
...	Feb 8 1200-Feb 9 0600	18.0	8*
...	Feb 10 0600-Feb 10 1000	4.0	8
...	Feb 10 1600-Feb 11 0200	10.0	8
...	Apr 24 1400-Apr 24 2200	8.0	8
...	May 6 1800-May 7 0000	6.0	8
...	May 21 0000-May 21 0400	4.0	8
Jun 13 0118	Jun 13 0800-Jun 13 1200	4.0	8
...	Jun 25 0800-Jun 25 1400	6.0	8
...	Jun 26 1800-Jun 26 2200	4.0	8
...	Jun 28 1800-Jun 28 2200	4.0	8
...	Aug 5 0000-Aug 5 1000	10.0	8
...	Aug 6 1600-Aug 6 2000	4.0	8
...	Aug 7 0000-Aug 7 0800	8.0	8
...	Aug 18 1200-Aug 18 1800	6.0	8
...	Aug 27 0200-Aug 27 0800	6.0	8
...	Aug 28 1400-Aug 28 1800	4.0	8

Shock	Bi Interval	Duration	S/C
Oct 4 0541	Oct 5 0400-Oct 5 1200	8.0	8
...	Oct 10 1600-Oct 10 2000	4.0	8
...	Oct 17 0600-Oct 17 1000	4.0	8
...	Oct 17 1400-Oct 17 2000	6.0	8
...	Oct 19 0600-Oct 19 1200	6.0	8
...	Oct 21 0000-Oct 21 0800	8.0	8
...	Nov 3 1000-Nov 3 1600	6.0	8
...	Nov 11 0200-Nov 11 0800	6.0	8
Nov 11 1110	Nov 11 2200-Nov 12 0600	8.0	8
	Nov 12 1200-Nov 13 0400	16.0	8
...	Nov 26 0800-Nov 26 1200	4.0	8
...	Dec 9 0000-Dec 9 1400	14.0	8
...	Dec 25 1600-Dec 25 2000	4.0	8
1984			
...	Jan 5 1800-Jan 6 0000	6.0	8
...	Jan 18 1400-Jan 18 2000	6.0	8
...	Mar 8 2000-Mar 9 0200	6.0	8
...	Mar 18 1600-Mar 18 2000	4.0	8
...	Mar 19 0200-Mar 19 0600	4.0	8
...	Mar 20 1600-Mar 20 2200	6.0	8*
...	Mar 22 0000-Mar 22 0600	6.0	8
...	May 6 0600-May 6 1200	6.0	8
...	May 7 0000-May 7 0400	4.0	8
...	May 11 0400-May 11 0800	4.0	8
Jun 15 0433	Jun 17 0000-Jun 17 0400	4.0	8
...	Jun 28 2200-Jun 29 0200	4.0	8
...	Jul 12 0400-Jul 12 1000	6.0	8
...	Jul 22 1800-Jul 23 0000	6.0	8
...	Aug 7 0400-Aug 7 0800	4.0	8
...	Aug 13 0600-Aug 13 1200	6.0	8
...	Aug 16 0800-Aug 16 1200	4.0	8
...	Aug 17 1400-Aug 17 1800	4.0	8
...	Aug 28 0000-Aug 28 0400	4.0	8
1985			
...	Jan 16 2000-Jan 17 0000	4.0	8
...	Jan 25 1200-Jan 25 1800	6.0	8
...	Feb 9 1400-Feb 9 2200	8.0	8
...	Feb 12 0400-Feb 12 1200	8.0	8
...	Feb 18 1800-Feb 18 2200	4.0	8
...	Feb 26 0000-Feb 26 0400	4.0	8
Mar 4 1827	Mar 6 1000-Mar 6 1400	4.0	8
...	Mar 23 0000-Mar 23 0400	4.0	8
...	Apr 4 1800-Apr 4 2200	4.0	8
...	Apr 10 0600-Apr 10 1000	4.0	8
...	Apr 24 0600-Apr 24 1000	4.0	8
...	May 11 0600-May 11 1600	10.0	8
...	Jun 3 1600-Jun 3 2200	6.0	8
...	Jun 27 0600-Jun 27 1600	10.0	8
...	Jul 12 1200-Jul 12 1800	6.0	8
...	Jul 20 1600-Jul 20 2200	6.0	8
Jul 22 1948	Jul 23 1400-Jul 23 2000	6.0	8
...	Aug 26 1400-Aug 26 2000	6.0	8
...	Oct 18 1200-Oct 18 1600	4.0	8
...	Nov 22 0600-Nov 22 1000	4.0	8
1986			
Feb 6 1313	Feb 8 0400-Feb 8 0800	4.0	8F
...	Feb 9 0600-Feb 9 0800	2.0	8*
Feb 9 1748	Feb 10 2000-Feb 11 0400	8.0	8
...	Apr 13 1200-Apr 13 1600	4.0	8
...	May 23 1000-May 23 2000	10.0	8
...	May 24 1600-May 24 2000	4.0	8
...	May 30 1200-May 30 1600	4.0	8
...	Jun 1 0800-Jun 1 1200	4.0	8
...	Jun 3 1000-Jun 3 1600	6.0	8
...	Jun 4 1600-Jun 5 0200	10.0	8
...	Jul 19 0800-Jul 19 1800	10.0	8
...	Aug 16 1200-Aug 16 1600	4.0	8
...	Aug 17 1600-Aug 17 2200	6.0	8
...	Aug 26 1800-Aug 27 0400	10.0	8
...	Sep 24 2000-Sep 25 0000	4.0	8
...	Nov 15 2000-Nov 16 0000	4.0	8
...	Dec 11 1200-Dec 11 1600	4.0	8

TABLE 2—*Continued*

Shock	Bi Interval	Duration	S/C
1987			
...	Jan 15 1000-Jan 15 1400	4.0	8
...	Jan 16 0200-Jan 16 1000	8.0	8
...	Jan 26 0400-Jan 26 1000	6.0	8
...	Apr 2 2200-Apr 3 0200	4.0	8
...	Apr 3 2200-Apr 4 0400	6.0	8
...	Apr 11 0800-Apr 11 1200	4.0	8
...	Apr 14 1600-Apr 14 2200	6.0	8
...	Apr 26 1800-Apr 26 2200	4.0	8
...	May 24 1800-May 25 0600	12.0	8F
...	Jun 2 0800-Jun 2 1200	4.0	8
...	Jun 14 0800-Jun 14 1400	6.0	8
...	Jun 30 1600-Jun 30 2200	6.0	8
...	Jul 11 1400-Jul 11 2000	6.0	8
...	Jul 24 1200-Jul 24 1800	6.0	8
...	Aug 5 0800-Aug 5 1600	8.0	8
...	Aug 29 0400-Aug 29 0800	4.0	8
Aug 29 1107	Aug 29 1600-Aug 29 2000	4.0	8
	Aug 30 1200-Aug 30 1800	6.0	8
Sep 10 1134	Sep 11 1800-Sep 11 2200	4.0	8
...	Sep 26 2200-Sep 27 0400	6.0	8
...	Oct 7 1600-Oct 8 0600	14.0	8
...	Oct 19 0800-Oct 19 1600	8.0	8
...	Oct 31 0800-Oct 31 1200	4.0	8
...	Nov 12 1000-Nov 12 1600	6.0	8
...	Nov 23 0400-Nov 23 1000	6.0	8
Dec 9 1941	Dec 11 2000-Dec 12 0200	6.0	8
Dec 28 2020	Dec 30 0000-Dec 30 1000	10.0	8*
1988			
Jan 13 2330	Jan 14 0600-Jan 14 1100	5.0	8C
	Jan 14 1900-Jan 15 0900	14.0	8C
...	Jan 17 1600-Jan 17 2200	6.0	8
...	Jan 26 0600-Jan 26 1000	4.0	8
...	Feb 7 0400-Feb 7 0800	4.0	8
...	Feb 8 1200-Feb 9 0600	18.0	8
...	Feb 9 1200-Feb 9 1600	4.0	8
...	Feb 10 1800-Feb 11 0000	6.0	8
...	Feb 11 1400-Feb 11 2200	8.0	8
Feb 22 0904	Feb 22 1600-Feb 22 2200	6.0	8
...	Mar 4 0400-Mar 4 0800	4.0	8
...	Mar 17 0800-Mar 17 1200	4.0	8
...	Mar 19 1400-Mar 19 2200	8.0	8
Mar 27 1347	Mar 29 0600-Mar 29 1000	4.0	8
...	Apr 25 1000-Apr 25 1400	4.0	8
...	Apr 27 1200-Apr 27 1600	4.0	8
...	Apr 28 2000-Apr 29 0200	6.0	8
May 6 0428	May 6 1000-May 6 1600	6.0	8
...	May 10 2200-May 11 0400	6.0	8
May 16 1635	May 18 0200-May 18 1000	8.0	8
...	May 22 2200-May 23 0400	6.0	8
...	Jun 1 1600-Jun 1 2200	6.0	8
...	Jun 18 0000-Jun 18 0400	4.0	8
Jul 5 1558	Jul 7 1200-Jul 7 1800	6.0	8
...	Jul 8 1600-Jul 9 0200	10.0	8
...	Jul 12 1600-Jul 12 2200	6.0	8
...	Jul 15 0200-Jul 15 0800	6.0	8
...	Jul 27 0000-Jul 27 0600	6.0	8
...	Aug 13 0600-Aug 13 1000	4.0	8
...	Aug 17 1600-Aug 17 2000	4.0	8
...	Aug 20 0200-Aug 20 0600	4.0	8
Aug 25 0932	Aug 26 0800-Aug 26 1200	4.0	8
...	Sep 13 1200-Sep 13 1800	6.0	8
...	Sep 14 1800-Sep 15 0000	6.0	8
...	Sep 15 1800-Sep 16 0000	6.0	8*
...	Sep 23 0600-Sep 23 1000	4.0	8
Oct 6 0038	Oct 7 2000-Oct 8 0200	6.0	8
Oct 10 0232	Oct 11 0000-Oct 11 0400	4.0	8
...	Oct 20 1600-Oct 20 2000	4.0	8
...	Oct 29 1200-Oct 29 2200	10.0	8
Oct 30 2001	Nov 1 1800-Nov 1 2200	4.0	8
...	Nov 3 1200-Nov 3 1600	4.0	8
...	Nov 4 1600-Nov 4 2200	6.0	8
Nov 11 0753	Nov 13 0600-Nov 13 1000	4.0	8*
...	Nov 26 1600-Nov 26 2000	4.0	8
...	Nov 29 0000-Nov 29 0400	4.0	8
...	Dec 7 1200-Dec 7 1800	6.0	8
Dec 22 1645	Dec 22 2000-Dec 23 0400	8.0	8*
	Dec 23 1400-Dec 24 0200	12.0	8*
...	Dec 30 1400-Dec 30 2000	6.0	8
...	Dec 31 1400-Dec 31 2000	6.0	8
1989			
...	Jan 1 1600-Jan 1 2000	4.0	8
...	Jan 3 1600-Jan 3 2200	6.0	8
Jan 11 1206	Jan 12 0200-Jan 12 1600	14.0	8
...	Jan 13 0200-Jan 13 0600	4.0	8
Jan 13 1326	Jan 13 1800-Jan 14 0200	8.0	8
...	Jan 14 0600-Jan 14 1600	10.0	8
...	Jan 30 2200-Jan 31 0200	4.0	8
...	Feb 6 2200-Feb 7 0400	6.0	8
...	Feb 7 1000-Feb 7 1400	4.0	8
Mar 2 0247	Mar 3 0800-Mar 3 1600	8.0	8
	Mar 4 0200-Mar 4 1000	8.0	8
...	Mar 15 1200-Mar 15 1600	4.0	8
Mar 17 0658	Mar 17 1000-Mar 17 2000	10.0	8*
...	Apr 2 1400-Apr 2 1800	4.0	8
Apr 13 2224	Apr 14 1800-Apr 14 2000	2.0	8*
Apr 24 2307	Apr 25 0400-Apr 25 0800	4.0	8
May 20 1545	May 20 1600-May 21 0800	16.0	8
May 23 1346	May 23 1800-May 23 2200	4.0	8
...	Jun 2 1800-Jun 2 2200	4.0	8
...	Jun 3 1800-Jun 3 2200	4.0	8
...	Jun 4 1600-Jun 4 2000	4.0	8
...	Jun 12 0400-Jun 12 0800	4.0	8
Jun 14 0107	Jun 14 1000-Jun 14 1400	4.0	8
	Jun 14 1800-Jun 15 0000	6.0	8
	Jun 15 2000-Jun 16 0200	6.0	8
...	Jun 17 1000-Jun 17 1600	6.0	8
...	Jun 27 2000-Jun 28 0600	10.0	8
...	Aug 4 1400-Aug 4 2000	6.0	8
...	Aug 7 0400-Aug 7 1000	6.0	8
Aug 14 0613	Aug 15 0400-Aug 15 2000	16.0	8*F
...	Aug 28 0000-Aug 28 0600	6.0	8*F
...	Aug 28 1800-Aug 28 2200	4.0	8*F
...	Sep 11 1600-Sep 11 2000	4.0	8
Sep 12 1228	Sep 12 2200-Sep 13 0000	2.0	8*
Sep 22 0742	Sep 23 1400-Sep 23 2000	6.0	8
Sep 26 0544	Sep 26 1800-Sep 27 0000	6.0	8
...	Oct 8 2000-Oct 9 0200	6.0	8
...	Oct 15 0800-Oct 15 1200	4.0	8
Oct 20 0916	Oct 21 1200-Oct 21 2000	8.0	8*F
Nov 9 0054	Nov 9 0200-Nov 9 1200	10.0	8*
Nov 11 1410	Nov 13 0800-Nov 13 1400	6.0	8
...	Nov 14 1400-Nov 14 2000	6.0	8
...	Nov 15 0200-Nov 15 1200	10.0	8
...	Nov 15 1800-Nov 16 0400	10.0	8
...	Nov 25 1800-Nov 26 0200	8.0	8
Nov 28 0743	Nov 29 1000-Nov 29 1200	2.0	8*F
Dec 22 0022	Dec 22 1800-Dec 23 0000	6.0	8
Dec 29 0655	Dec 29 1600-Dec 29 2200	6.0	8
	Dec 30 0200-Dec 30 0800	6.0	8

NOTES.—M $\geq$ 35 keV BIF; G = BHF; C = Magnetic Cloud; 8 = GSFC *IMP 8* BIF (asterisk denotes three or more energy channels); 3 = GSFC *ISEE 3/ICE* BIF (asterisk denotes three or more energy channels); He = He abundance enhancement; F = Forbush decrease.

TABLE 3

Intervals with Two or More CME Signatures

Shock	Bi Interval	Duration	Sigs.
1978			
Aug 18 1242	Aug 19 0300-Aug 19 0600	3.00	8MHe
Aug 27 0246	Aug 27 1800-Aug 28 1300	19.00	8MGC
...	Sep 9 1230-Sep 9 2000	7.50	83
Sep 10 0105	Sep 10 0200-Sep 10 1800	16.00	83GHe
Sep 29 0301	Sep 29 0915-Sep 30 1100	25.75	3*MGCHe
Oct 4 0047	Oct 4 0600-Oct 5 0730	25.50	8*3*
...	Oct 11 1245-Oct 11 1600	3.25	83
...	Oct 11 2145-Oct 12 0445	7.00	83
...	Oct 18 2000-Oct 19 0400	8.00	83
...	Oct 21 0400-Oct 21 1230	8.50	83
...	Oct 22 0200-Oct 22 0615	4.25	83
Oct 29 1116	Oct 29 2200-Oct 31 1200	38.00	8MGC
...	Nov 10 1745-Nov 10 2200	4.25	8*3F
Nov 12 0100	Nov 12 1430-Nov 14 1015	43.75	8*3*MGHe
...	Nov 14 1600-Nov 14 2200	6.00	83
...	Nov 16 1045-Nov 16 2115	10.50	83
...	Dec 7 0600-Dec 7 0815	2.25	83
...	Dec 7 1600-Dec 7 2015	4.25	83
Dec 14 0127	Dec 15 2315-Dec 16 0700	7.75	3M
Dec 17 1258	Dec 18 0530-Dec 18 1230	7.00	83
1979			
Jan 2 2100	Jan 2 2300-Jan 5 0000	49.00	83*MHe
Jan 6 0032	Jan 6 2200-Jan 9 0000	50.00	83MG
Jan 22 1900	Jan 23 1745-Jan 24 0250	9.08	3G
Jan 25 0045	Jan 25 0115-Jan 25 1200	10.75	3G
...	Feb 10 1415-Feb 10 1800	3.75	83
Feb 11 0148	Feb 12 1200-Feb 14 2015	56.25	83*M
Feb 21 0302	Feb 21 0400-Feb 21 0730	3.50	83
	Feb 21 1500-Feb 22 0700	16.00	83GHe
...	Feb 23 0900-Feb 23 1900	10.00	83MGF
...	Feb 23 2215-Feb 24 0800	9.75	83F
Mar 6 0818	Mar 6 1015-Mar 6 1400	3.75	83
	Mar 7 2100-Mar 8 0200	5.00	83
...	Mar 8 1730-Mar 9 0400	10.50	83
Mar 9 0808	Mar 9 1800-Mar 10 1030	16.50	8*3*G
...	Mar 19 1000-Mar 19 1800	8.00	83He
Mar 21 1251	Mar 21 1800-Mar 22 0515	11.25	83
Mar 22 0826	Mar 22 1630-Mar 23 0730	15.00	MG
Apr 1 2150	Apr 3 0000-Apr 3 1000	10.00	83M
Apr 3 1001	Apr 3 1930-Apr 5 0115	29.75	8*3*GC
Apr 5 0156	Apr 5 0950-Apr 6 1500	29.17	3*MG
...	Apr 8 1515-Apr 9 0445	13.50	3*G
...	Apr 9 1135-Apr 9 1415	2.67	3G
...	Apr 14 2215-Apr 15 0215	4.00	83
Apr 24 2358	Apr 25 1110-Apr 26 1445	27.58	83*GF
...	May 9 2200-May 10 0615	8.25	83*
...	May 10 1000-May 10 1615	6.25	83
...	May 12 0300-May 12 0600	3.00	83
...	May 20 1600-May 20 2015	4.25	83
May 29 1851	May 29 2030-May 31 1400	41.50	8*3*MG
...	Jun 2 0200-Jun 2 0430	2.50	83
...	Jun 3 0200-Jun 3 1100	9.00	8*3
...	Jun 4 2145-Jun 5 0600	8.25	83
Jun 6 1927	Jun 6 1615-Jun 7 0800	15.75	83*GF
...	Jun 13 2200-Jun 14 0245	4.75	83
...	Jun 15 0730-Jun 15 2000	12.50	83
...	Jun 18 2000-Jun 18 2215	2.25	83
...	Jul 10 0530-Jul 10 0815	2.75	8*3
Jul 12 1240	Jul 13 0115-Jul 13 0515	4.00	83
	Jul 13 2200-Jul 14 0230	4.50	83
	Jul 14 1600-Jul 14 1800	2.00	83
...	Jul 24 1400-Jul 24 1930	5.50	83
...	Aug 4 1000-Aug 4 1545	5.75	83
...	Aug 7 1215-Aug 7 1600	3.75	83
...	Aug 8 2200-Aug 9 0115	3.25	83
...	Aug 9 1445-Aug 9 1945	5.00	83
Aug 13 0611	Aug 14 0715-Aug 14 1400	6.75	83
...	Aug 16 2215-Aug 17 1200	13.75	83
...	Aug 17 1700-Aug 18 0315	10.25	83F
Aug 29 0459	Aug 29 1800-Aug 30 1630	22.50	83*G
Aug 31 0510	Sep 1 1530-Sep 1 2000	4.50	83
...	Sep 9 0815-Sep 9 2200	13.75	83M
...	Sep 10 0730-Sep 10 2000	12.50	83M
...	Sep 14 2115-Sep 15 0030	3.25	83
Sep 17 0448	Sep 18 0800-Sep 20 0615	46.25	3*MGCHe
...	Sep 26 1115-Sep 26 2000	8.75	83
...	Oct 4 1005-Oct 5 1000	23.92	8G
Oct 6 1120	Oct 7 0125-Oct 7 0840	7.25	83GF
	Oct 7 2000-Oct 8 0330	7.50	8*3*F
Nov 11 0225	Nov 11 2230-Nov 13 2145	47.25	83G
...	Nov 14 0715-Nov 14 1600	8.75	83
...	Nov 23 1300-Nov 24 0130	12.50	83G
...	Nov 25 1000-Nov 26 2200	36.00	83M
...	Nov 29 0600-Nov 29 2045	14.75	83*
Nov 30 0738	Nov 30 1330-Dec 1 0030	11.00	3G
...	Dec 2 1200-Dec 2 1800	6.00	3M
...	Dec 3 0630-Dec 5 0700	48.50	GC
...	Dec 23 0600-Dec 24 1145	29.75	83
Dec 30 1000	Dec 30 1600-Dec 30 2030	4.50	83
	Dec 31 1715-Jan 1 2100	27.75	83G
1980			
Jan 13 0510	Jan 13 1700-Jan 14 2200	29.00	83MG
...	Jan 15 0530-Jan 15 2200	16.50	8G
Jan 17 0512	Jan 17 1600-Jan 18 0110	9.17	8G
...	Jan 25 0900-Jan 25 2300	14.00	8G
Jan 25 1109	Jan 27 0530-Jan 27 1600	10.50	83*
Feb 9 0338	Feb 10 2300-Feb 11 0515	6.25	83
...	Feb 11 1900-Feb 12 0115	6.25	83
...	Feb 12 2000-Feb 13 0200	6.00	83
...	Feb 13 1200-Feb 13 1530	3.50	83
Feb 14 0309	Feb 14 1400-Feb 15 0045	10.75	G3*
Feb 15 1235	Feb 15 0300-Feb 17 0900	54.00	3MGC
	Feb 17 1230-Feb 18 0800	19.50	3*G
...	Feb 18 1600-Feb 19 0030	8.50	83
...	Feb 21 0500-Feb 21 1600	11.00	8G
Mar 19 0617	Mar 19 1500-Mar 21 1900	52.00	MGC
...	Mar 30 0900-Mar 30 1915	10.25	83
Mar 31 1749	Apr 1 0130-Apr 2 1745	40.25	8*3*MGF
Apr 6 1059	Apr 6 2000-Apr 6 2310	3.17	3G
Apr 9 0508	Apr 9 1000-Apr 11 1400	52.00	83G
...	Apr 12 1330-Apr 12 1800	4.50	83
...	Apr 15 0600-Apr 15 1200	6.00	83
...	Apr 25 1800-Apr 25 2130	3.50	83
May 7 0803	May 8 1200-May 10 0000	36.00	8MG
...	May 10 0500-May 10 1030	5.50	8G
...	May 10 1600-May 10 2200	6.00	83
...	May 19 0800-May 19 2200	14.00	8G
...	May 21 2200-May 22 0200	4.00	8G
May 29 1832	May 30 1800-May 31 1615	22.25	83G
May 31 2137	May 31 2200-Jun 1 0630	8.50	83G
	Jun 1 1015-Jun 1 1645	6.50	83
...	Jun 3 0400-Jun 3 1315	9.25	83
Jun 4 0300	Jun 5 0700-Jun 5 1900	12.00	3M
Jun 10 1627	Jun 11 1300-Jun 14 0700	66.00	8MG
Jun 24 0248	Jun 24 0800-Jun 25 0700	23.00	83GF
	Jun 25 1400-Jun 25 2000	6.00	83F
...	Jun 26 1830-Jun 27 0345	9.25	3G
...	Jun 27 1430-Jun 27 2000	5.50	83
...	Jun 29 2230-Jun 30 0700	8.50	83
...	Jul 2 2140-Jul 3 0640	9.00	3MG
...	Jul 22 2000-Jul 23 0300	7.00	83
Jul 25 1111	Jul 26 1200-Jul 27 0200	14.00	3MGF
Jul 27 0157	Jul 28 0040-Jul 30 0515	52.58	3G
Aug 6 0010	Aug 6 1200-Aug 6 2200	10.00	8G
Aug 11 1656	Aug 13 0115-Aug 13 0600	4.75	83
	Aug 13 1600-Aug 14 0600	14.00	83MG
Aug 16 1240	Aug 16 2200-Aug 17 1700	19.00	8G
Aug 19 1024	Aug 19 1430-Aug 22 0100	58.50	83*M
Sep 3 1336	Sep 4 0015-Sep 4 2000	19.75	3*G
...	Sep 11 0930-Sep 12 0815	22.75	8G
Sep 13 0900	Sep 12 2000-Sep 13 2100	25.00	83MG
Sep 20 0139	Sep 21 1000-Sep 21 1515	5.25	83
...	Sep 22 0400-Sep 22 0715	3.25	83
...	Sep 24 0715-Sep 24 1345	6.50	3G
...	Oct 6 1130-Oct 7 0630	19.00	83*M

TABLE 3—*Continued*

Shock	Bi Interval	Duration	Sigs.
...	Oct 7 1130-Oct 7 2130	10.00	83
...	Oct 10 0550-Oct 10 1700	11.17	8G
Oct 14 1953	Oct 15 0600-Oct 15 2200	16.00	8*3*MG
Oct 18 0114	Oct 19 1600-Oct 19 2015	4.25	83
...	Nov 3 1400-Nov 3 2115	7.25	83
Nov 9 1122	Nov 9 1330-Nov 10 0645	17.25	83*
...	Nov 29 0730-Nov 30 0030	17.00	3*GF
...	Nov 30 2000-Dec 1 1830	22.50	3*GF
...	Dec 5 2000-Dec 5 2245	2.75	83
Dec 11 1009	Dec 11 1910-Dec 14 0200	54.83	3MG
...	Dec 17 0400-Dec 17 0815	4.25	83
...	Dec 17 1745-Dec 18 0200	8.25	83
Dec 19 0456	Dec 19 1200-Dec 20 1400	26.00	GCF
	Dec 20 1950-Dec 20 2300	3.17	8MGF
...	Dec 21 1200-Dec 21 2000	8.00	83*
Dec 25 0552	Dec 27 0200-Dec 30 0300	73.00	3*G
Dec 30 0738	Dec 31 0800-Dec 31 1530	7.50	83
1981			
Jan 29 0646	Jan 29 0800-Jan 31 0300	43.00	83*G
Feb 6 0847	Feb 6 1745-Feb 8 1830	48.75	83*MGC
Feb 8 1345	Feb 8 2200-Feb 9 0600	8.00	8G
...	Feb 20 1000-Feb 21 0300	17.00	8*3*MG
...	Feb 21 1000-Feb 22 1630	30.50	83MG
Mar 5 0535	Mar 5 1300-Mar 8 0000	59.00	83MG
Mar 7 0153	Mar 7 1730-Mar 8 0000	6.50	83*MG
	Mar 8 0545-Mar 8 0830	2.75	83
Mar 12 1824	Mar 14 1500-Mar 15 1600	25.00	8G
...	Mar 20 1300-Mar 20 1800	5.00	83
...	Mar 21 0645-Mar 21 1345	7.00	83
Apr 7 1954	Apr 8 1800-Apr 9 0900	15.00	3M
Apr 12 2120	Apr 13 1900-Apr 14 1300	18.00	8*3*MG
Apr 18 1503	Apr 19 1130-Apr 20 0340	16.17	3*G
...	Apr 24 0715-Apr 24 1600	8.75	83
Apr 26 0813	Apr 26 2200-Apr 27 0145	3.75	83*
...	May 4 1845-May 5 2015	25.50	83
...	May 7 0315-May 7 0700	3.75	83
...	May 9 0800-May 9 1400	6.00	83
May 10 2208	May 11 0800-May 14 1820	82.33	3*MG
May 15 0252	May 15 0530-May 16 0510	23.67	3*GF
May 17 2302	May 18 0750-May 19 1400	30.17	83*G
...	May 24 2330-May 25 0800	8.50	3*M
...	May 25 1545-May 27 1530	47.75	3*MG
Jun 7 0823	Jun 7 2015-Jun 8 2330	27.25	3G
...	Jun 14 1045-Jun 15 0000	13.25	83*MG
...	Jun 16 0800-Jun 16 1245	4.75	83
Jun 21 0600	Jun 21 2100-Jun 22 0100	4.00	3M
...	Jun 28 0730-Jun 28 1200	4.50	83
...	Jun 28 2000-Jun 28 2245	2.75	83
Jun 29 0610	Jun 29 0830-Jun 29 1200	3.50	83
	Jun 30 0400-Jun 30 1245	8.75	83
...	Jul 8 1000-Jul 8 1530	5.50	83
...	Jul 9 1830-Jul 10 0200	7.50	83
...	Jul 10 1800-Jul 11 0930	15.50	83
Jul 17 0802	Jul 17 2100-Jul 19 2300	50.00	3*MG
Jul 23 0646	Jul 22 1800-Jul 24 1000	40.00	8*3*GF
Jul 25 1322	Jul 25 1930-Jul 27 2000	48.50	3*MG
...	Aug 7 1200-Aug 7 2000	8.00	8G
Aug 10 0434	Aug 10 0020-Aug 11 1030	34.17	3G
...	Aug 15 0200-Aug 15 0800	6.00	83
...	Aug 16 1715-Aug 17 0515	12.00	83
...	Aug 20 0000-Aug 20 0800	8.00	83
...	Aug 29 1100-Aug 30 0130	14.50	83
Aug 30 2222	Aug 31 1200-Sep 1 1015	22.25	83
...	Sep 2 0530-Sep 2 0845	3.25	83
...	Sep 2 1415-Sep 3 0200	11.75	83
Sep 8 2146	Sep 10 0400-Sep 10 1000	6.00	83
...	Sep 11 0900-Sep 11 1800	9.00	83G
Sep 18 1912	Sep 19 0700-Sep 20 0530	22.50	3MC
...	Sep 22 1800-Sep 24 0000	30.00	83*G
...	Sep 26 0720-Sep 27 0500	21.67	8G
Oct 2 2022	Oct 3 0015-Oct 4 0100	24.75	83GF
	Oct 4 2000-Oct 5 0600	10.00	83F
...	Oct 6 1400-Oct 6 2100	7.00	83G
Oct 10 1434	Oct 11 0000-Oct 11 2245	22.75	3G
Oct 13 2240	Oct 15 1400-Oct 15 2300	9.00	3G
...	Oct 18 0000-Oct 18 0800	8.00	83*
Oct 20 1309	Oct 20 1800-Oct 20 2200	4.00	83
...	Nov 1 2000-Nov 1 2300	3.00	83
...	Nov 8 1600-Nov 9 0400	12.00	83
Nov 11 1238	Nov 11 2300-Nov 14 0400	53.00	83*GF
...	Nov 21 0700-Nov 22 1800	35.00	83*MG
Nov 25 0229	Nov 25 1030-Nov 26 0000	13.50	83G
...	Nov 29 0600-Nov 29 1200	6.00	83
...	Dec 4 0400-Dec 4 0700	3.00	83
...	Dec 4 2300-Dec 5 0700	8.00	83
Dec 8 1400	Dec 9 2010-Dec 10 0200	5.83	83*G
Dec 12 0144	Dec 12 2300-Dec 13 1730	18.50	3G
...	Dec 15 0530-Dec 15 1800	12.50	3G
...	Dec 19 0700-Dec 19 1400	7.00	83
Dec 29 0455	Dec 29 1200-Dec 30 0200	14.00	83G
	Dec 30 1700-Jan 1 0900	40.00	3G
1982			
...	Jan 10 0600-Jan 11 0200	20.00	83
...	Jan 12 0330-Jan 12 0630	3.00	83
Jan 13 0412	Jan 13 1700-Jan 14 0950	16.83	3G
Jan 29 1745	Jan 31 1350-Feb 1 1030	20.67	3*MGF
Feb 3 0129	Feb 3 2200-Feb 4 0600	8.00	3G
...	Feb 5 0400-Feb 5 1800	14.00	83*MG
...	Feb 6 0200-Feb 6 2000	18.00	3G
...	Feb 9 0745-Feb 10 0000	16.25	8*3MG
Feb 11 1313	Feb 11 2200-Feb 15 0530	79.50	83MGF
Feb 21 0727	Feb 23 0100-Feb 23 1300	12.00	8G
Mar 1 1138	Mar 1 1300-Mar 1 2215	9.25	3G
...	Mar 9 0000-Mar 9 2150	21.83	8G
...	Mar 14 2100-Mar 15 0700	10.00	3G
...	Mar 17 0150-Mar 17 1320	11.50	3G
...	Mar 19 1000-Mar 19 1930	9.50	3MG
...	Mar 21 0500-Mar 21 1615	11.25	83*
...	Mar 22 2000-Mar 23 0000	4.00	83G
Apr 1 1305	Apr 3 0550-Apr 3 1600	10.17	3G
...	Apr 9 1230-Apr 11 0830	44.00	83G
...	Apr 13 0800-Apr 13 1700	9.00	83G
...	Apr 13 2100-Apr 14 0545	8.75	83
...	Apr 24 0300-Apr 24 0600	3.00	83
Apr 24 2016	Apr 25 0100-Apr 27 0915	56.25	83MGF
...	Apr 27 2200-Apr 28 0800	10.00	83
...	May 4 1200-May 4 1400	2.00	83
...	May 5 1400-May 5 2015	6.25	83
...	May 6 0900-May 6 1400	5.00	83
...	Jun 1 1000-Jun 1 1615	6.25	83
Jun 9 0040	Jun 9 0430-Jun 9 2000	15.50	3*G
Jun 12 1443	Jun 13 1300-Jun 14 0200	13.00	83G
...	Jun 16 0400-Jun 16 0730	3.50	83
...	Jun 23 1000-Jun 23 1415	4.25	3G
...	Jun 24 0500-Jun 24 0800	3.00	83
...	Jul 9 0745-Jul 9 1200	4.25	83
Jul 13 1617	Jul 13 2330-Jul 16 1440	63.17	83*G
Jul 16 1519	Jul 16 2330-Jul 17 1530	16.00	3*G
...	Jul 18 1445-Jul 19 0515	14.50	3G
Aug 6 1836	Aug 6 2200-Aug 7 2300	25.00	83G
...	Aug 27 1000-Aug 28 0300	17.00	83G
...	Aug 28 0830-Aug 28 1400	5.50	83*
Sep 5 2250	Sep 6 0450-Sep 8 1400	57.17	3GF
Sep 9 0101	Sep 10 0230-Sep 10 1915	16.75	8G
Sep 21 0339	Sep 21 1130-Sep 22 0900	21.50	8*3*G
	Sep 22 1530-Sep 22 2115	5.75	8*3*G
...	Sep 23 0600-Sep 24 0400	22.00	83G
...	Sep 24 2345-Sep 25 0200	2.25	83
Sep 25 2030	Sep 25 0900-Sep 26 1800	33.00	83C
Sep 26 1033	Sep 26 1930-Sep 27 0000	4.50	83
...	Oct 4 1230-Oct 4 2245	10.25	83
...	Oct 28 0400-Oct 28 1400	10.00	83
...	Oct 29 0600-Oct 29 1245	6.75	83
...	Oct 30 1800-Oct 31 0200	8.00	83
Oct 31 1338	Nov 1 0100-Nov 1 1600	15.00	83*
	Nov 2 1400-Nov 3 0300	13.00	83
...	Nov 4 0000-Nov 4 1200	12.00	83
Dec 7 0329	Dec 8 0100-Dec 8 0615	5.25	83
...	Dec 15 0730-Dec 17 1000	50.50	83*C
Dec 17 0806	Dec 18 1530-Dec 19 0400	12.50	83*
Dec 19 0254	Dec 19 0800-Dec 19 1700	9.00	83*

tion, rather than >4 hr in Table 2. The various signatures associated with each interval are indicated in the manner of Table 2. We identify 293 distinct events, corresponding to a rate of ~0.18 events day^{-1} (66 events per year, consistent with the rate of CMEs predicted by Gosling et al. [1992] to be encountered by an observer in the ecliptic). Their total combined duration is 198 days, corresponding to ~12% of the observation time. Figure 11 shows frequency distributions of the total event durations and of the durations of the various signatures from which they are derived. The event durations range from <2 hr to ~80 hr, with a mean of 16.2 ± 15.7 hr. The distribution falls off approximately exponentially with increasing duration from 2 to ~30 hr (scale size < 0.4 AU) and in addition shows a population of events around 40–60 hr duration (scale size ~0.5–0.7 AU). Around 10% of bidirectional regions have scale sizes greater than 0.5 AU while ~50% have durations of 1–10 hr, corresponding to ~0.01–0.1 AU.

Considering the various signatures, the >35 keV BIFs (15.0 ± 11.9 hr) and BHFs (19.2 ± 16.8 hr) have similar durations to the complete events. On the other hand, the mean duration of the 16 magnetic clouds in this interval is 29 ± 13 hr. This implies that magnetic clouds (as identified by Burlaga et al. 1981; Klein & Burlaga 1982; Zhang & Burlaga 1988; Lepping et al. 1990) only include the longer duration bidirectional regions, as Gosling (1990) has also pointed out. This is also evident from Figure 8 where bidirectional intervals associated with magnetic field rotations resembling those in magnetic clouds are apparent which have not been identified as magnetic clouds but which are apparently a similar, but smaller scale, phenomenon.

The *IMP 8* and *ISEE 3/ICE* BIFs have rather shorter durations (3.6 ± 3.1 hr and 5.9 ± 5.1 hr, respectively). This may reflect the tendency for energetic ion bidirectionality to be intermittent within a given bidirectional region. For example, Figure 12 shows *ISEE 3/ICE* observations on 1979 September 17–20 in a similar format to Figure 1. The magnetic field structure from 0800 UT September 18 to 2300 UT September 19, exhibiting smooth variations in field direction, has been identified by Zhang & Burlaga (1988) as a magnetic cloud forming the driver of a shock at 1000 UT on September 17. A BHF was reported by Gosling et al. (1987) on September 17–18, but a high background produced by the intense energetic particle fluxes (panel 5) prevented the start and stop times from being determined exactly. However, there is an indication that BHFs may have commenced before the arrival of the cloud. Marsden et al. (1987) reported a >35 keV BIF within the magnetic cloud at 1500–2100 UT September 18 (which however they classified as being unrelated with both a rotational field structure and a shock driver). Neugebauer & Alexander (1991) identified a helium abundance enhancement at 0945–1750 UT on September 19, within the trailing edge of the cloud. Hence, various signatures of shock drivers/CMEs on September 17–19 have been reported, but not at exactly the same locations.

It is evident from the seventh panel that 1–4 MeV amu^{-1} ion bidirectionality is present only intermittently for episodes of a few hours at a time from ~0815 UT on September 18, close to cloud entry, through to ~0615 UT on September 20, after cloud passage. The corresponding intervals identified in the

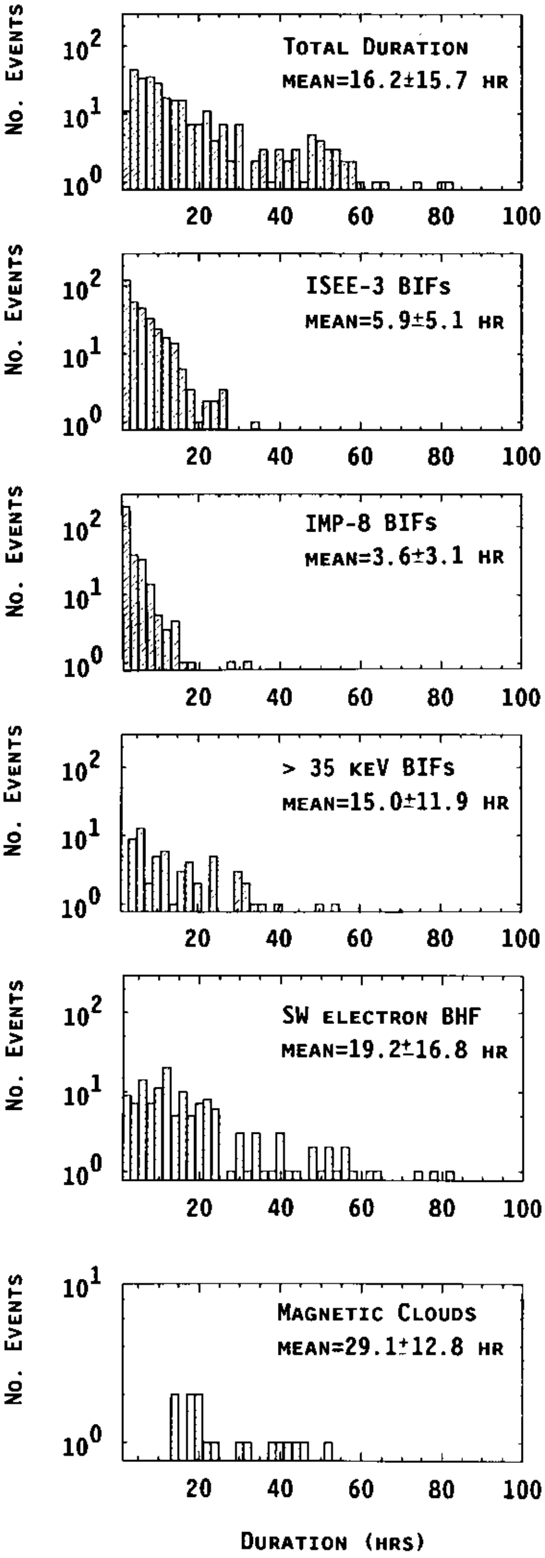

FIG. 11.—Frequency distributions of CME (bidirectional particle/magnetic cloud) region durations in 1978–1982 obtained from *IMP 8* and *ISEE 3/ICF* ~1 MeV amu^{-1} BIFs, >35 keV BIFs, solar wind electron BHFs, and magnetic clouds. The top panel shows the overall durations of these regions while the lower panels give distributions for the individual signatures.

TABLE 4

ISEE 3/ICE Bidirectional Intervals (1984–1991)

Bi Interval	Duration (hr)	
1984		
< Jan 18 0430 - Jan 18 0830	>4.00	
Feb 8 0430 - Feb 8 0915	4.75	
< Feb 9 0030 - Feb 9 0630	>6.00	*
Feb 16 0230 - Feb 16 0630	4.00	
Feb 26 0630 ->Feb 26 1030	>4.00	
Feb 27 0130 ->Feb 27 1045	>9.25	
< Feb 28 2230 - Feb 29 0330	>5.00	*
Mar 2 0630 - Mar 2 1030	4.00	
Mar 4 0830 ->Mar 4 1430	>6.00	
< Mar 20 2315 - Mar 21 0415	>5.00	
Apr 10 0400 - Apr 10 0915	5.25	*
Apr 20 2230 - Apr 21 0430	6.00	
Apr 30 2215 - May 1 0245	4.50	*
May 3 0145 - May 3 0615	4.50	
< May 5 2230 - May 6 1145	>13.25	*
May 17 0000 - May 17 2215	22.25	
May 31 0615 - May 31 1015	4.00	
Jun 3 0615 - Jun 3 1015	4.00	
Jun 6 0945 - Jun 6 1800	8.25	
Jun 7 1815 - Jun 7 2215	4.00	
Jun 23 0345 - Jun 23 1615	12.50	*
Jul 4 0415 - Jul 4 1015	6.00	
< Jul 9 0015 - Jul 9 0615	>6.00	
Jul 25 0615 - Jul 25 1815	12.00	
Aug 20 0215 ->Aug 20 0815	>6.00	
Aug 21 0215 ->Aug 21 0815	>6.00	
< Aug 25 2215 - Aug 26 0215	>4.00	
Aug 27 0045 - Aug 27 0615	5.50	*
Sep 5 0415 - Sep 5 0815	4.00	
Nov 6 0215 ->Nov 6 0815	>6.00	
Dec 1 0400 - Dec 1 0745	3.75	
Dec 5 1215 ->Dec 5 1615	>4.00	
Dec 15 0815 ->Dec 15 1215	>4.00	
Dec 30 0415 - Dec 30 1015	6.00	
1985		
Jan 1 1215 ->Jan 2 1415	>26.00	
< Feb 10 1415 - Feb 10 1815	>4.00	
< Mar 9 1100 - Mar 9 1500	4.00	
Apr 28 2300 - Apr 29 0330	4.50	*
< May 1 1700 ->May 2 1600	>23.00	
< Jul 7 1700 - Jul 7 2100	>4.00	
Jul 8 1500 - Jul 8 1900	4.00	
< Jul 11 0300 ->Jul 11 2100	>18.00	
Jul 12 1700 - Jul 12 2100	4.00	
< Jul 14 0300 - Jul 14 1500	>14.00	
Jul 19 0545 - Jul 19 1030	4.75	
Jul 22 0100 - Jul 22 1700	16.00	
Aug 4 0700 - Aug 4 1300	6.00	
Sep 21 0700 - Sep 21 1300	6.00	
< Sep 22 0100 - Sep 22 0500	>4.00	
Sep 23 0500 - Sep 23 1100	6.00	
Sep 26 0700 - Sep 26 1100	4.00	
< Oct 7 1100 - Oct 7 1700	>6.00	
Nov 4 0700 - Nov 4 1100	4.00	
< Nov 12 1500 ->Nov 14 1500	>48.00	
< Dec 1 0100 ->Dec 1 0700	>6.00	
Dec 3 0500 - Dec 3 1100	6.00	
< Dec 4 0900 - Dec 4 1300	>4.00	
< Dec 9 0100 ->Dec 9 0500	>4.00	
< Dec 31 0100 ->Dec 31 0700	>6.00	
1986		
< Feb 14 1100 ->Feb 14 1500	>4.00	
May 5 1430 - May 5 1830	4.00	
May 6 1230 ->May 6 2030	>8.00	
May 10 1430 ->May 10 1830	>4.00	
Jun 8 1230 - Jun 8 1700	4.50	
Jul 7 0430 - Jul 7 0830	4.00	
Jul 8 1230 - Jul 9 0630	18.00	
< Jul 15 0230 - Jul 15 0830	>6.00	
< Jul 23 1030 ->Jul 23 1430	>4.00	
Aug 23 1630 ->Aug 23 2030	>4.00	
Oct 19 1230 - Oct 19 1630	4.00	
1987		
May 30 1300 - May 30 1815	5.25	
< Aug 20 0930 ->Aug 20 1530	>6.00	
< Sep 5 1030 - Sep 5 1415	>3.75	
Sep 6 1145 ->Sep 6 1530	>3.75	
< Sep 8 0530 - Sep 8 1930	>14.00	
Sep 9 1130 ->Sep 9 1530	>4.00	
Sep 11 1730 - Sep 11 2130	4.00	
Sep 12 1130 ->Sep 12 1530	>4.00	
Sep 13 1130 ->Sep 13 1530	>4.00	
< Oct 1 0330 ->Oct 1 1130	>8.00	
< Oct 3 0530 ->Oct 3 1130	>6.00	
< Oct 8 0330 ->Oct 8 0930	>6.00	
Oct 13 0330 - Oct 13 0730	4.00	
Oct 14 0330 ->Oct 14 0730	>4.00	
< Oct 29 0330 - Oct 29 0730	>4.00	
Nov 2 0730 ->Nov 2 1130	>4.00	
< Nov 14 0330 - Nov 14 0730	>4.00	
< Dec 7 0330 - Dec 7 0730	>4.00	
1988		
< Jan 2 0330 - Jan 2 0815	>4.75	
< Jan 10 0530 - Jan 10 0945	>4.25	
< Jan 13 1730 ->Jan 13 2130	>4.00	
< Feb 14 0730 ->Feb 14 1130	>4.00	
< Feb 16 0530 ->Feb 16 1130	>6.00	
< Mar 5 0530 ->Mar 5 0930	>4.00	
< Mar 28 0530 - Mar 28 0930	>4.00	
< Mar 30 0530 ->Mar 30 0930	>4.00	
< Apr 2 0530 - Apr 2 0930	>4.00	
< Apr 20 0530 - Apr 20 0930	>4.00	
< Apr 22 0530 - Apr 22 1130	>6.00	
< May 6 0530 - May 6 1130	>6.00	
May 7 0730 ->May 7 1330	>6.00	
< May 22 0530 - May 22 0930	>4.00	
Jun 14 0330 - Jun 14 0930	6.00	
Jun 29 0730 - Jun 29 1130	4.00	
Jul 9 0530 - Jul 9 1130	6.00	
Jul 10 1330 - Jul 10 1730	4.00	
< Jul 18 0330 - Jul 18 0930	>6.00	
Sep 1 1330 ->Sep 1 1730	>4.00	
< Sep 5 0130 - Sep 5 0530	>4.00	
< Nov 9 1130 - Nov 9 1730	>6.00	
Nov 18 0530 ->Nov 18 0930	>4.00	
< Dec 20 1100 ->Dec 20 1700	>6.00	
< Dec 29 0300 - Dec 29 0700	>4.00	
1989		
< Jan 7 0630 - Jan 7 1130	>5.00	
< Jan 8 0600 ->Jan 8 1015	>4.25	G
< Jan 21 0500 ->Jan 21 1015	>5.25	G
< Mar 14 0700 ->Mar 14 1000	>3.00	
< Mar 20 1515 ->Mar 20 1745	>2.50	
< Mar 23 0630 - Mar 23 1100	>4.50	
< Mar 30 0545 - Mar 30 1100	>5.25	
< May 24 0845 ->May 24 1100	>2.25	
< May 28 1730 - May 29 2345	>30.25	G
May 30 0945 - May 30 1615	6.50	
Jun 3 1030 ->Jun 4 1300	>2.50	
< Jun 4 0445 ->Jun 4 1200	>7.25	
Jun 21 0745 ->Jun 21 1245	>5.00	
Jun 24 0700 - Jun 24 1845	11.75	GM
Jun 25 0000 ->Jun 25 1245	>12.75	M
< Jul 6 0715 ->Jul 6 1045	>3.50	
Aug 18 0830 ->Aug 18 2100	>12.50	GM*
Aug 19 0815 ->Aug 19 1345	>5.50	G*
Aug 20 0515 ->Aug 20 0830	>3.25	
Aug 21 0800 ->Aug 21 1245	>4.75	GM*
< Aug 22 0245 - Aug 22 0845	>6.00	G
Aug 26 0215 - Aug 26 0930	7.25	G*
< Aug 28 0200 - Aug 28 0800	>6.00	
< Sep 2 0200 - Sep 2 1200	>10.00	

TABLE 4—*Continued*

Bi Interval	Duration (hr)	
Sep 20 0500 - Sep 20 0915	4.25	
< Oct 17 0300 - Oct 17 0715	>4.25	
< Oct 28 0615 ->Oct 28 1000	>3.75	
Nov 4 0500 - Nov 4 0915	4.25	
< Nov 17 1230 ->Nov 17 1800	>5.50	
< Nov 23 0430 - Nov 23 1500	>10.50	
Nov 26 0615 ->Nov 26 1600	>9.75	
1990		
< Jan 27 0500 - Jan 27 0900	>4.00	
< Feb 17 0900 ->Feb 17 1300	>4.00	
< Mar 13 1500 ->Mar 13 2100	>6.00	
Apr 5 1300 - Apr 5 1700	4.00	
< Apr 23 1300 ->Apr 23 2100	>8.00	
< Apr 27 1300 - Apr 27 1700	>4.00	
Apr 29 1300 ->Apr 29 2100	>8.00	
Apr 30 0500 - Apr 30 0900	4.00	
< May 1 1700 ->May 1 2100	>4.00	
< May 6 1700 ->May 6 2100	>4.00	
< May 14 1900 ->May 14 2100	>2.00	
< May 15 1700 ->May 15 1900	>2.00	
< May 16 1700 ->May 16 2300	>6.00	
May 19 1500 ->May 19 1900	>4.00	
< May 27 2100 ->May 28 2100	>24.00	*
< Jun 4 0300 - Jun 4 1100	>8.00	
Jun 11 0700 - Jun 11 1100	4.00	
< Jun 13 0300 ->Jun 13 0900	>6.00	
< Jun 18 0500 ->Jun 18 1100	>6.00	
Jul 6 1300 ->Jul 6 1900	>6.00	
Jul 9 0500 ->Jul 9 0900	>4.00	
Jul 13 1500 - Jul 13 1900	4.00	
< Jul 14 0900 - Jul 14 1300	>4.00	
Jul 25 0500 ->Jul 25 0900	>4.00	
< Jul 27 0100 ->Jul 27 0900	>8.00	
Jul 31 1500 ->Jul 31 2300	>8.00	
< Aug 13 0900 - Aug 13 1300	>4.00	
< Aug 15 0900 - Aug 15 1300	>4.00	
< Aug 25 1500 ->Aug 25 2300	>8.00	
Aug 31 1700 ->Aug 31 2100	>4.00	
< Sep 9 1300 ->Sep 9 2100	>8.00	
< Sep 10 1500 ->Sep 10 2100	>6.00	
< Oct 13 1100 ->Oct 13 1500	>4.00	
< Oct 28 1100 ->Oct 28 1500	>4.00	
Dec 2 1300 ->Dec 2 1900	>6.00	
< Dec 28 0500 ->Dec 28 0900	>4.00	
1991		
< Feb 6 1700 ->Feb 6 2100	>4.00	
< Feb 11 1500 ->Feb 11 2100	>6.00	

NOTES.—M = >35 keV BIF; G = BHF; Asterisk denotes three or more energy channels.

survey are indicated in the top panel. Representative pie plots showing sectored ion intensities during 15 minute intervals starting at the times indicated are shown at the bottom of the figure, and they illustrate the clear changes in the ion distribution. The intermittent disappearance of bidirectional flow in the vicinity of the magnetic cloud does not occur simply when the magnetic field has a large angle to the ecliptic and falls well outside the instrument viewing cone. For example, bidirectionality is clearly evident in the distribution for 1000 UT on September 18 (DOY 261) when the magnetic field was inclined $\sim 60°$ south of the ecliptic while at 2100 UT on September 19 (DOY 262), a nearly isotropic distribution occurred when the field was $\sim 35°$ south, only 10° outside of the VLET viewing cone. Furthermore, Marsden et al. (1987) also identified the discrete episode of bidirectional flow during the second half of September 18, even though they were able to measure the three-dimensional ion distribution. Thus the intermittent bidirectionality does not arise from instrumental limitations and suggests that bidirectional ions were present only in restricted regions within this magnetic cloud. The bottom panel, showing the plasma temperature, also supports a spatial interpretation since the BIFs show some association with local minima in the plasma temperature. In this event, the BIFs tend to occur toward the edges of the CME and are absent in the center, but this does not appear to be a general rule, based on a limited review of our observations (see, for example, Fig. 1, where the strongest bidirectionality occurs in the center of the bidirectional region) and the events illustrated by Marsden et al. (1987), Tranquille et al. (1987) and Sanderson et al. (1990) which also show evidence of intermittent bidirectionality. (We note that the BIF intervals indicated by these authors generally encompass these times so that their mean durations are longer than those obtained in this study.)

The main points illustrated here are that each interval of bidirectional ion flow is not necessarily associated with an individual CME (which we here assume to be indicated by the magnetic cloud signature) and that bidirectional flows are not always observed throughout a CME, and hence may not be used alone to define the extent of a CME. The fact that BIFs are observed intermittently within CMEs also suggests that some of the very brief BIFs identified may occur within CMEs of longer duration, and that it is also possible that bidirectional ion flows may be absent within some CMEs (such as the event in Figs. 9 and 10).

Within the bidirectional intervals in Table 3, BHFs are observed for the greatest duration, 110.4 days, corresponding to $\sim 57\%$ of the total bidirectional interval duration. *ISEE 3/ICE* BIFs are observed for 82 days ($\sim 42\%$), while *IMP 8* BIFs are seen for 43 days ($\sim 22\%$) which however approximates to the *ISEE 3/ICE* rate if the lower data coverage is taken into account (~ 96 days, $\sim 49\%$). The >35 keV BIFs are observed for 37.5 days ($\sim 19\%$), and magnetic clouds for 19.4 days ($\sim 10\%$) (again indicating that magnetic clouds are observed in association with only a small subset of bidirectional intervals).

3.7. *BIFs Identified at ISEE 3/ICE from 1984 to 1991*

The final list (Table 4) shows BIFs with durations ≥ 4 hr observed by *ISEE 3/ICE* following injection into heliocentric orbit in 1984 until 1991 February. Various limitations of these data were noted above in § 2. During 1984–1989, the spacecraft advanced ahead of Earth by $\sim 90°$ in heliolongitude (von

Rosenvinge et al. 1986) so that by 1989, it lay off of the west limb of the Sun at ~1 AU heliocentric distance. In this location, BIFs may be directly correlated with CMEs ejected from the western limb of the Sun. However, a study of this topic is beyond the scope of this paper. Where BIFs in 1989 are associated with (although not necessarily over exactly the same intervals) bidirectional solar wind heat fluxes noted by J. T. Gosling (1990, private communication), this is indicated by "G" while "M" indicates events with >35 keV bidirectional ion streaming (T. R. Sanderson 1990, private communication). Asterisks indicate events seen in three or more energy channels.

4. SUMMARY AND DISCUSSION

Some 4000 intervals of bidirectional field-aligned ~1 MeV amu^{-1} ion flows, ranging in duration from 15 minutes to over 60 hr (scale sizes from ~0.003 to ~0.7 AU), have been identified in the solar wind at 1 AU from 1973 to 1991. The occurrence rate falls off approximately exponentially with duration, with an *e*-folding time of ~4 hr. The occurrence of bidirectional flows shows a dependence on solar activity levels. BIFs are observed ~12% of the time at solar maximum, falling to ~5% at solar minimum. These rates are reasonably consistent with the solar cycle variation of bidirectional heat fluxes found by Gosling et al. (1992). At solar minimum, BIFs with durations > 4 hr are observed at a rate of <0.1 day^{-1}, rising to ~0.2–0.3 day^{-1} at solar maximum. Of these events, ~33% are observed <2 days following shocks and/or SSCs, so the majority of BIFs are not associated with shocks. The identified periods show reasonable (~80% or better) but not exact agreement with previously reported intervals of bidirectional >35 keV ions and bidirectional solar wind electron heat fluxes, and with magnetic clouds, helium enhancements, and Forbush decreases. These phenomena have been previously interpreted as possible interplanetary signatures of coronal mass ejections. In the remaining 20% of CME signatures, around half have low ion fluxes so that the ion flow cannot be determined, while the ions in the other events do not show bidirectional streaming because of the dominance of unidirectional-streaming or isotropic solar or shock-accelerated ions. Additional BIF intervals have also been found during which these other signatures have not been reported. In addition to the factors mentioned above, this lack of complete agreement may also reflect data selection criteria. (For example, Marsden et al. [1987] considered only >35 keV BIF events at least 3 hr in duration.) Nonetheless, there is clear evidence that these various signatures do not correspond exactly, as indicated for example by the intermittent bidirectionality within the magnetic cloud in Figure 12. We note that Zwickl et al. (1983) observed a similar patchy distribution of regions of enhanced helium abundances in shock drivers and in some cases, the absence of particular characteristic signatures.

Considering all the various CME signatures together for events in 1978–1982 (around solar maximum), we find that regions in which these signatures are observed occur at a rate of ~0.18 day^{-1}, and have mean durations of 16.3 ± 15.8 hr, equivalent to scale sizes of ~0.20 ± 0.19 AU. This variation indicates that these regions have a wide range of scale sizes in the solar wind. The regions identified as magnetic clouds, with durations of tens of hours, represent only the infrequent, longer duration events.

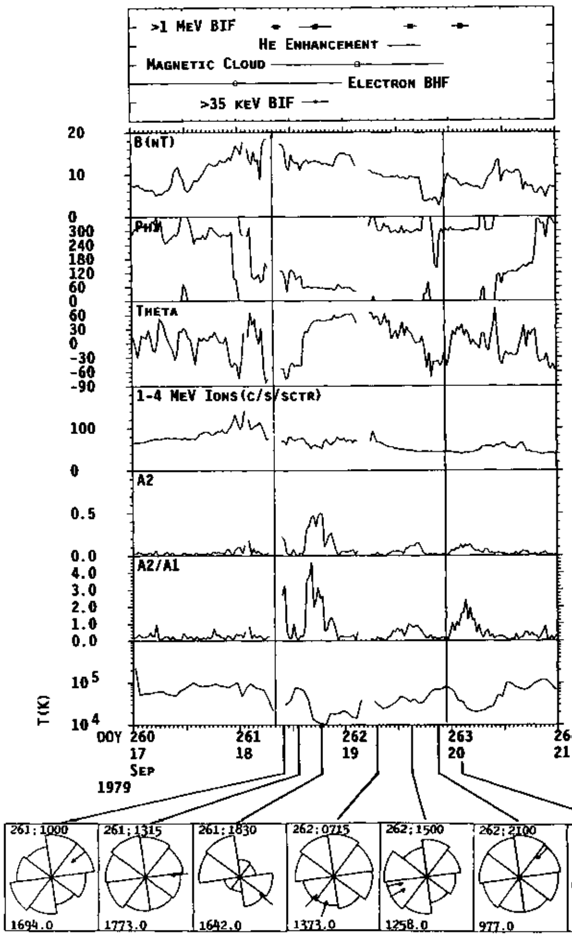

FIG. 12.—Intermittent 1–4 MeV amu^{-1} bidirectional ion flow associated with a magnetic cloud on 1979 September 18–19.

Differences in the regions over which the various signatures are observed, and changes in the strength of bidirectional flows within these regions, are to be expected if the particles are traveling (and influenced by propagation conditions) along magnetic field lines within a large-scale magnetic structure for distances of several AU. For example, if the mean-free path were somehow to be reduced on a magnetic field loop within such a structure, then the bidirectional flow along that loop would eventually be destroyed on time scales of the order of the structure size divided by the particle speed. It is possible that solar wind heat flux electrons, >35 keV and >1 MeV amu^{-1} ions sample different regions of the structure due to their different speeds and hence are influenced to varying degrees by propagation conditions along a given field line. In this case, bidirectionality may not be observed at the spacecraft over exactly the same region for each type of particle. Also, in flux-rope-like magnetic fields characteristic of some CMEs, in particular magnetic clouds (Burlaga 1988; Lepping et al. 1990), particle propagation may be significantly different along axial magnetic field lines in the center of the flux rope than along helical magnetic field lines at the periphery. Changes in ion streaming may also result from particle injection into a CME (Sarris and Krimigis 1982; Richardson, Cane, & von Rosenvinge 1991; Richardson, Farrugia, & Burlaga, 1991) (indicating the presence of field lines rooted at the Sun [Kahler & Reames 1991]). Overall, a careful study of the various interplanetary CME signatures is required to clarify how they are related and their implications for our understanding of the structure of CMEs and the origin of bidirectional particle flows in general. We do conclude, however, that there is not a one-to-one association between the BIFs identified in this study and individual CMEs. While BIFs indicate regions where CMEs may be located, for the reasons given above the detection (or otherwise) of a BIF alone cannot confirm that a CME is (or is not) present.

This work is supported by NASA grant NGR 21-002-316. Reference to bidirectional solar wind heat flux and >35 keV ion event lists compiled by J. T. Gosling and T. R. Sanderson, respectively, is gratefully acknowledged. We appreciate comments on the manuscript by H. V. Cane and by the referee.

REFERENCES

Balogh, A., & Erdös, G. 1983, Planet. Space Sci., 31, 1389
Borrini, G., Gosling, J. T., Bame, S. J., & Feldman, W. C. 1982a, J. Geophys. Res., 87, 4365
———. 1982b, J. Geophys. Res., 87, 7370
Burlaga, L. F. 1988, J. Geophys. Res., 93, 7217
Burlaga, L. F., Sittler, E., Mariani, F., & Schwenn, R. 1981, J. Geophys. Res., 86, 6673
Cocconi, G., Gold, T., Greisen, K., Hayakawa, S., & Morrison, P. 1958, Nuovo Cimento Soc. Ital. Fis., 8, 161
Couzens, D. A., & King, J. H. 1986, Interplanetary Medium Data Book, Suppl. 3, 1977–85, NSSDC/WDCA (Greenbelt: GSFC)
Decker, R. B. 1983, J. Geophys. Res., 88, 9959
Farrugia, C. J., Burlaga, L. F., Osherovich, V. A., Richardson, I. G., Freeman, M. P., Lepping, R. P., & Lazarus, A. 1992, J. Geophys. Res., In press
Gold, T. 1959, J. Geophys. Res., 64, 1665
Gosling, J. T. 1990, AGU Geophys. Monog., 58, Physics of Magnetic Flux Ropes, ed. C. T. Russell, E. R. Priest, & L. C. Lee (Washington, DC: AGU) 343
Gosling, J. T., Baker, D. N., Bame, S. J., Feldman, W. C., Zwickl, R. D., & Smith, E. J. 1987, J. Geophys. Res., 92, 8519
Gosling, J. T., Bame, S. J., McComas, D. J., & Phillips, J. L. 1990, Geophys. Res. Lett., 17, 901
Gosling, J. T., McComas, D. J., Phillips, J. L., & Bame, S. J. 1992, J. Geophys. Res., 97, 6531
Hundhausen, A. J. 1988, Proc. 6th Internat. Solar Wind Conf., ed. V. Pizzo, T. E. Holzer, & D. G. Sime NCAR/TN-306+Proc., 181
Kahler, S. K. 1987, Rev. Geophys., 25, 663
———.1988, Proc. 6th Internat. Solar Wind Conf., ed. V. Pizzo, T. E. Holzer, & D. G. Sime, NCAR/TN-306+Proc, 215
Kahler, S. K., & Reames, D. V. 1991, J. Geophys. Res., 96, 9419
Klein, L. W., & Burlaga, L. F. 1982, J. Geophys. Res., 87, 613
Kutchko, F. J., Briggs, P. R., & Armstrong, T. R. 1982, J. Geophys. Res., 87, 1419
Lepping, R. P., Jones, J. A., & Burlaga, L. F. 1990, J. Geophys. Res., 95, 11957
Marsden, R. G., Sanderson, T. R., Tranquille, C., Wenzel, K.-P., & Smith, E. J. 1987, J. Geophys. Res., 92, 11009
McGuire, R. E., von Rosenvinge, T. T., & McDonald, F. B. 1986, ApJ, 301, 938
Morrison, P. 1954, Phys. Rev., 95, 641
Neugebauer, M., & Alexander, C. J. 1991, J. Geophys. Res., 96, 9409
Palmer, I. D., Allum, F. R., & Singer, S. 1978, J. Geophys. Res., 83, 75
Piddington, J. R. 1958, Phys. Rev., 119, 589
Rao, U. R., McCracken, K. G., & Bukata, R. P., J. Geophys. Res., 1967, 72, 4325
Richardson, I. G., Cane, H. V., & von Rosenvinge, T. T. 1991, J. Geophys. Res., 96, 7853
Richardson, I. G., Farrugia, C. J., & Burlaga, L. F. 1991, Proc. 22d. Internat. Cosmic-Ray Conf. (Dublin), 3, 597
Richardson, I. G., & Reames, D. V. 1991, Proc. 22d. Internat. Cosmic Ray Conf. (Dublin), 3, 292
St. Cyr, O. C., & Burkepile, J. T. 1990, Tech. Note NCARTN-352+STR (Boulder: NCAR)
Sanderson, T. R., Reinhard, R., & Wenzel, K.-P. 1981, J. Geophys. Res., 86, 4425
Sanderson, T. R., Marsden, R. G., Reinhard, R., Wenzel, K.-P., & Smith, E. J. 1983, Geophys. Res. Lett., 10, 916
Sanderson, T. R., Beeck, J., Marsden, R. G., Tranquille, C., Wenzel, K.-P., McKibben, R. B., & Smith, E. J. 1990, Proc. 21st Internat. Cosmic-Ray Conf. (Adelaide), 6, 255
Sarris, E. T., & Krimigis, S. M. Geophys. Res. Lett., 9, 167, 1982
Solar Geophysical Data. 1990, No. 549 (Boulder, CO: NOAA Environmental Data & Information Service)
Tranquille, C., Sanderson, T. R., Marsden, R. G., & Wenzel, K.-P. 1987, J. Geophys. Res., 92, 6
van Nes, P., Reinhard, R., Sanderson, T. R., Wenzel, K.-P., & Zwickl, R. D. 1984, J. Geophys. Res., 89, 2122
von Rosenvinge, T. T., McDonald, F. B., Trainor, J. H., Van Hollebeke, M. A. I., & Fisk, L. A. 1978, IEEE Trans. Geosci. Elec., GE-16(3), 208
Webb, D. F. 1991, Adv. Space Res., 11, (1)37
Wilson, R. M., & Hildner, E. 1986, J. Geophys. Res., 91, 5867, 1986
Zhang, G., & Burlaga, L. F. 1988, J. Geophys. Res., 93, 2511
Zwickl, R. D., & Webber, W. R. 1976, Nucl. Instrum. Meth., 138, 191
Zwickl, R. D., Asbridge, J. R., Bame, S. J., Feldman, W. C., Gosling, J. T., & Smith, E. J. 1983, Solar Wind Five, NASA CP-2280, 711